

TIME DIVISION ACCESS FEASIBILITY STUDY
MODULATION AND SYNCHRONIZATION CONSIDERATIONS

Contract No. NASW-1216

Prepared by: JJ Bisaga
G. F. Dooley

P. C. Jain
P. C. Jain

Reviewed by: JJ Bisaga
J. J. Bisaga, Program Manager

N. MacGregor
N. MacGregor
Director, Aerospace Sciences Division

Approved by: R. M. Hultberg
R. M. Hultberg
Vice-President and
Director of Operations

COMMUNICATION SYSTEMS, INCORPORATED

FALLS CHURCH, VIRGINIA

TABLE OF CONTENTS

Section		Page
1	INTRODUCTION.....	1-1
2	TECHNICAL ANALYSIS.....	2-1
	2.1 General.....	2-1
	2.2 Synchronization.....	2-3
	2.2.1 Network Timing.....	2-3
	2.2.2 Frame Synchronization Errors.....	2-5
	2.3 TDA Efficiency.....	2-5
	2.4 TDA System Figure of Merit and Optimization.....	2-6
	2.4.1 RF Synchronization.....	2-8
	2.4.2 Bit Synchronization.....	2-13
	2.4.3 Frame Synchronization.....	2-27
	2.4.4 Sample Calculation.....	2-38
3	CONCLUSIONS.....	3-1
	REFERENCES.....	R-1
Appendix		
A	ANALYSIS OF PSK DEMODULATOR FOR TDA SYSTEMS	A-1
	A.1 PSK Modulation.....	A-1
	A.2 Initial Conditions.....	A-4
	A.3 Acquisition Time.....	A-7

SECTION 1
INTRODUCTION

Much of the current planning for international communication satellite systems is oriented toward large capacity trunking systems (60 to 1000 voice channels) within the existing and planned, ground-based, international toll networks. That is, the satellite system provides large capacity transmission trunks between the ground-based switching or message centers. Satellites, however, are capable of providing a much more flexible service. In particular, communication satellites could support a small user access system, somewhat analogous to an exchange area switching system, wherein any station can communicate with any other station in the same geographical coverage area. The satellite could provide a large number of low capacity accesses and the system could accommodate a variety of configurations varying from full time interconnections of several voice channels between two ground stations to part-time interconnections of one voice channel or several telegraph channels between two ground stations.

The central technical difficulty in implementing such a system with satellites lies in developing an efficient and sufficiently flexible means of satellite access for a large number of ground stations, which will accommodate different transmission rates and provide controlled pseudo-random access to the system, without undue overall system complexity. Time division access, (TDA) offers considerable advantages under many conditions. The inherent flexibility of the time sharing approach makes it possible for any transmission station to address any or all receiving stations. A single transmitter

may thus divide the transmission time to obtain simultaneous communication with several different receivers. A further advantage of TDA for satellite access is that since the signals are never simultaneously present at the satellite repeater, there is no interference between signals, and power control of transmitters, in the usual sense, is unnecessary.

The purpose of this study is to investigate some of the problems relating to the technical feasibility of time division access. The objective was to develop an optimizing technique for a small user TDA system, i.e., a system consisting of a large number of small ground stations, each requiring only a low capacity (a few voice or telegraph channels).

A figure of merit is derived for a TDA system and it is shown that optimization of this figure of merit is equivalent to maximizing the number of accesses (providing that some other limitation does not take effect first) for a given received carrier to noise density ratio. The figure of merit includes the effects of RF, bit and frame synchronization efficiencies and effective energy per bit to noise density ratio. Various techniques are examined and their effect on the figure of merit is analyzed. Numerical examples are used to demonstrate the effects and their interrelationships in a quantitative manner.

SECTION 2
TECHNICAL ANALYSIS

2.1 GENERAL

Time Division Access (TDA) permits a number of ground stations to simultaneously use a common satellite repeater through time-sequencing of their transmissions. If there is no time overlap of the bursts arriving at the satellite, then the bursts are truly orthogonal and mutual interference is nonexistent. However, if excessive guard bands must be provided between bursts to allow for timing inaccuracy, then the efficiency of this technique is reduced.

The general frame diagram, shown in Figure 2-1(a), depicts the timing at the input to the satellite for N accesses. Figure 2-1(b) shows the diagram of a general transmitter assigned to the i th time slot and the required timing relationships. As shown in Figure 2-1(b), the input data, arriving at a rate of R_i , is stored in the buffer. At the proper time (determined by the path delay to the satellite, τ_i , and the desired time of arrival of the bursts at the satellite), the accumulated block of $R_i T_F$ symbols is gated to a modulator at a rate of $R_i \left(\frac{T_F}{T_i} \right)$ and transmitted to the satellite. If the timing relationships are correct, the data burst will arrive at the satellite at the beginning of time slot i at time $\left(t_o + T_{FS} + \sum_{j=1}^{i-1} T_j \right)$ and the burst will terminate at the end of time slot i at time $\left(t_o + T_{FS} + \sum_{j=1}^i T_j \right)$. This action is periodically repeated every T_F seconds.

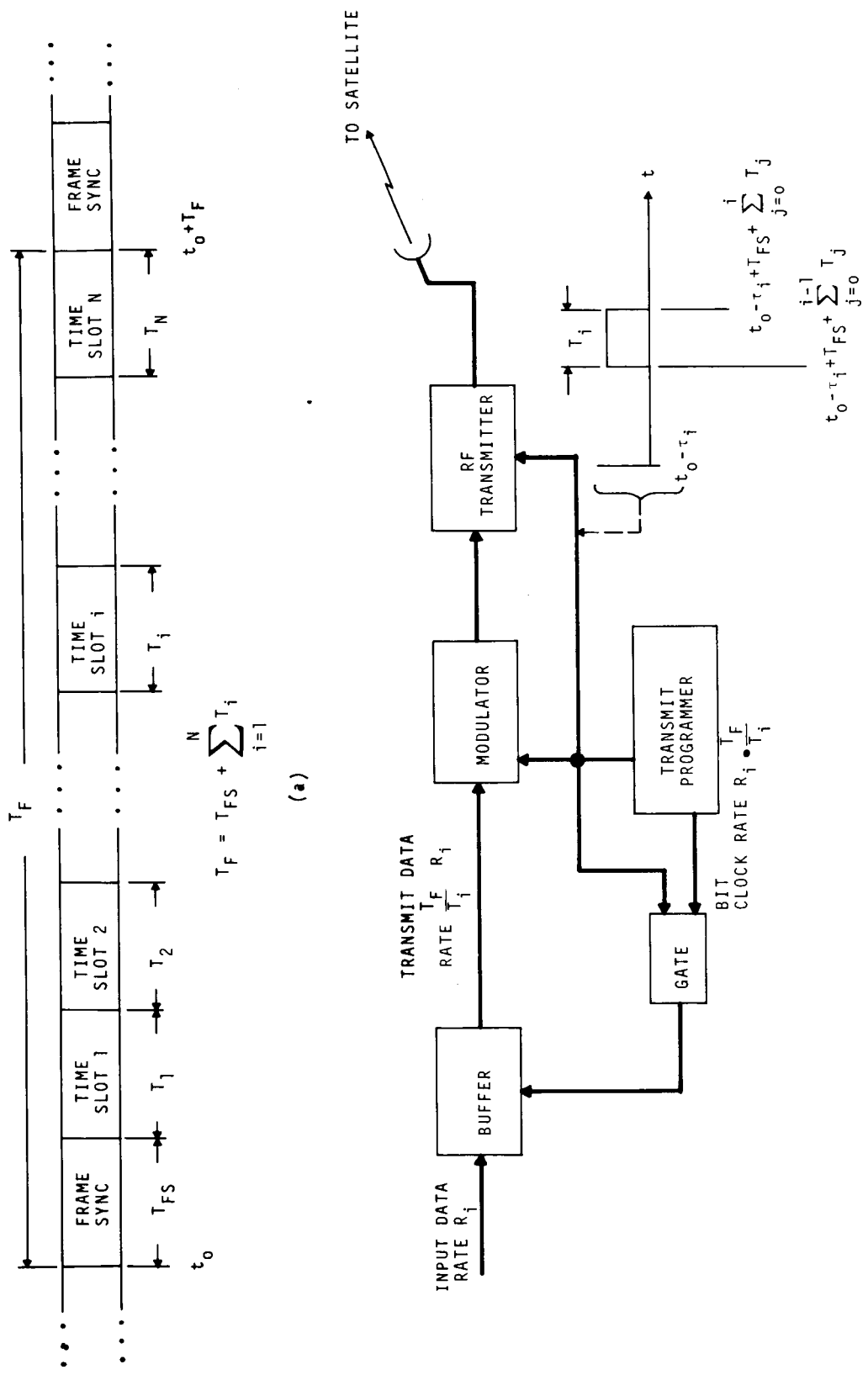


Figure 2-1. General Frame Diagram and Transmitter Block Diagram

2.2 SYNCHRONIZATION

As can be seen from the preceding description, the key to designing a TDA system lies in the precise time synchronization of the burst transmissions. In addition, because TDA, as considered in this study, is a digital transmission system, other forms of synchronization are required. In general, the various forms of synchronization required are as follows:

- a. Frame Synchronization - Overall network timing of the bursts from the different sources.
- b. RF Synchronization - Establishment of any RF frequency and phase necessary for demodulation.
- c. Symbol (or Bit) Synchronization - Establishment of a local receiver clock at the frequency and phase of the data stream within a burst.
- d. Word Synchronization - Establishment of the phase of a block of bits of the data stream within a burst.

Each of these forms of timing is not independent. For example, the symbol or bit synchronizer may be a part of the frame synchronizer and the word synchronizer. Additionally, if the number of blocks of data within a burst is an integral number, the word synchronizer may be a subsystem of the frame synchronizer. There are a number of ways to obtain each type of synchronization and the crux of the problem to be solved is the intelligent selection of a set of synchronization techniques which optimizes the average data rate for a given set of constraints.

Before discussing a general model for TDA systems and its optimization, a discussion of network timing is necessary.

2.2.1 Network Timing

Network timing to establish burst synchronization can originate either from the satellite itself or from one of the ground

stations, acting as the master station. The former approach suffers from the inherent drawback that once the frame length is fixed it cannot be changed, making the system inflexible. This approach is also nonadaptive in nature, as far as satellite power utilization is concerned. Sufficient power margin must be provided so that under worst conditions the timing information can be received by the smallest station. Another disadvantage of having the network timing originate from the satellite is the dependence of the overall system reliability on the reliability of the satellite timing source. To circumvent these drawbacks, network timing will be assumed, for the purposes of this study, to originate from one of the ground stations.

The timing can be continuous and transmitted in a form orthogonal with the data, or it may be a repetitive function, interlaced in time with bursts of data. For continuous transmission, unless a separate satellite repeater is used, there will be interaction between timing and data. Also, additional ground equipment will be required to separate timing and data, which will increase both satellite and ground station complexity and lower the system reliability. The method of transmitting timing information as a separate burst interlaced in time with data bursts does not suffer from the drawbacks of the continuous transmission mentioned. It makes efficient use of transmitter power and uses the same satellite equipment as the data, thereby not affecting the reliability of the system. Also no additional ground receiving equipment is required which may otherwise decrease ground station reliability. Finally, in a digital transmission system, continuous transmission of timing information is not required.

Therefore network timing will be assumed to originate from one of the ground stations, acting as a master station, and will be transmitted as a separate burst time shared with the data bursts.

2.2.2 Frame Synchronization Errors

There are several sources of frame synchronization (burst position) errors in a TDA system:

a. Measurement Error - When the time of occurrence of a signal perturbed with noise is measured, the error committed is dependent on the signal, noise and the measurement method.

b. Translation Error - If the time of occurrence of an event is stored (e.g., by means of a shift register or counter) and later employed to initiate an action, a translation error occurs which is determined by the accuracy of the clock.

c. Burst Position System Error - The burst position system is assumed to be a closed loop servo. Thus, a deterministic burst position error will exist which is a function of the loop parameters and the time derivatives of the round-trip delay between a ground station and the satellite. The burst position system also has a statistical error, which is a function of the measurement and translation errors as well as the servo characteristics.

These errors can cause system degradation and thus necessitate a guard band between adjacent bursts sufficiently wide that the total burst position error will not, with a high probability, result in an overlap of bursts and hence loss of data. These errors are analyzed in Paragraph 2.4.3.1.

2.3 TDA EFFICIENCY

The efficiency of a TDA system can, in general, be defined as:

$$\eta = \frac{\text{total data time in a frame interval}}{\text{frame interval}} \quad (2-1)$$

$$= \frac{T_F - T_{FS} - T_G - T_{BS} - T_{RF}}{T_F} \quad (2-2)$$

where T_F = Frame interval

T_{FS} = Interval for frame synchronization

T_G = Total guard intervals

T_{BS} = Total time for bit synchronization

T_{RF} = Total time for RF synchronization (carrier acquisition)

The total TDA efficiency, η , may be rewritten as:

$$\eta = \frac{T_F - T_{FS} - T_G}{T_F} \cdot \frac{(T_F - T_{FS} - T_G) - T_{BS}}{(T_F - T_{FS} - T_G)} \cdot \frac{(T_F - T_{FS} - T_G - T_{BS}) - T_{RF}}{(T_F - T_{FS} - T_G - T_{BS})} = \eta_F \cdot \eta_{BS} \cdot \eta_{RF} \quad (2-3)$$

where η_F = Frame efficiency, which accounts for the fraction of total time devoted to framing and burst synchronization.

η_{BS} = Bit synchronization efficiency, which accounts for the fraction of remaining time devoted to bit synchronization.

η_{RF} = RF efficiency, which accounts for the fraction of the remaining time devoted to RF carrier recovery.

Thus, to achieve a high overall system efficiency, the individual efficiencies η_F , η_{BS} , and η_{RF} must be high.

2.4 TDA SYSTEM FIGURE OF MERIT AND OPTIMIZATION

This paragraph defines a figure of merit for a TDA system which is a function of the preceding efficiencies as well as the theoretical energy per bit to noise density ratio and its degradation due to imperfect generation of the local data clock. Techniques are then derived to permit optimization of this figure of merit. For a given RF demodulation scheme, the output error rate of a digital transmission system is dependent on the ratio of signal energy per bit to noise density, E_b/N_o (Reference 1). Assuming perfect bit synchronization at the receiver, the theoretical data rate which can be received is given by:

$$R_T = \frac{1}{\tau_B} = \frac{C/N_o}{E_b/N_o} \quad (2-4)$$

where C/N_o is the received average carrier power to noise density ratio and τ_B is the bit duration. In a practical system, however, perfect bit synchronization is difficult to achieve. Because of noise, a local clock derived from the input data stream at the receiver will not be in phase with the data. The resulting degradation in effective E_b/N_o can be approximated by including a factor of $\cos^2 \theta$ where θ is the phase error. Thus to maintain the desired error rate, the required energy per bit to noise density ratio would be $\frac{1}{\cos^2 \theta} \cdot E_b/N_o$; and the modified data rate

$$R = \frac{C/N_o}{E_b/N_o} \cdot \cos^2 \theta \quad (2-5)$$

Referring to Figure 2-1(b), the burst data rate, R , can also be related to the baseband data rate, R_i , as

$$R = R_i \frac{T_F}{T_i} \quad (2-6)$$

where T_i is the data interval per burst duration. That is,

$$T_i = \frac{1}{N} \left[T_F - T_{FS} - T_G - T_{BS} - T_{RF} \right] \quad (2-7)$$

where N is the total number of equal data time slots in the frame. With the aid of Equations (2-2) and (2-7), the output data rate can be written explicitly as:

$$R = R_i \frac{N}{\eta} \quad (2-8)$$

The total number of accesses N of a TDA system can finally be obtained by combining Equations (2-5) and (2-8).

$$N = \frac{C/N_o}{R_i} \cdot \frac{\eta \cos^2 \theta}{E_b/N_o} \quad (2-9)$$

For a given base band data rate, R_i , and a received carrier to noise density ratio; C/N_o , a figure of merit for a TDA system can be defined as

$$F = \eta \frac{\cos^2 \theta}{E_b/N_0} \quad (2-10)$$

or more explicitly with the aid of Equation (2-3) as

$$F = \frac{\eta_{RF}}{E_b/N_0} \cdot \eta_{BS} \cos^2 \theta \cdot \eta_F \quad (2-11)$$

The concept of a figure of merit can be suitably used as a basis for optimization of a TDA system. It can be conveniently separated into three separate terms, each of which can be maximized independently.

2.4.1 RF Synchronization

The term $\frac{\eta_{RF}}{E_b/N_0}$ contained in Equation (2-11) is a function of the modulation scheme and carrier synchronization technique. To determine the number of symbols required at the beginning of a burst to establish the RF phase and frequency for different modulation schemes, it is useful to consider a constant error rate for the system and represent the RF efficiency

$$\eta_{RF} = 1 - \frac{T_{RF}}{T_F - T_{FS} - T_G - T_{BS}} \quad (2-12)$$

as

$$\eta_{RF} = 1 - \frac{n_{RF}}{n_B} \quad (2-13)$$

where n_{RF} is the total number of symbols per burst required for RF synchronization and n_B is the total number of symbols per burst. For a given burst interval, the number of symbols required for RF synchronization n_{RF} , will vary for different modulation schemes. Also the quantity E_b/N_0 must be obtained from the error rate performance of various digital modulation techniques.

It is well known that if a coherent PSK modulation scheme is employed, a clean version of the carrier must be provided at

the beginning of each burst for demodulation. The number of symbols required to establish the local phase of the reference carrier is determined in general by the method of synchronization and the required E_b/N_0 . Lindsey (Reference 2) has analyzed a self-synchronizing method in which the phase of the reference carrier is derived from the modulated signal by means of a squaring loop. Curves for error probability as a function of E_b/N_0 are also given by Lindsey, for different values of δ , which is a parameter defined essentially as the ratio of the data rate to the noise bandwidth of the phase lock loop. From these curves, one can easily construct curves for E_b/N_0 as a function of δ for constant error probabilities. Such a curve is shown in Figure 2-2 for an error probability of 10^{-4} .

The settling time of the loop is a function of the noise bandwidth of the loop (B_L) and the initial phase and frequency errors. It is derived in Appendix A as:

$$T_S = \frac{3.0}{B_L} \quad (2-14)$$

The number of symbols required for RF synchronization is:

$$n_{RF} = T_S \cdot R = \frac{3.0 \cdot R}{B_L} = 3.0 \delta \quad (2-15)$$

For example, if δ is in the range from 1 to 5, the number of sync symbols required is in the range from 3 to 15. The settling time of the loop, however, can be considerably reduced by employing a dual loop technique, analyzed in Appendix A. It is shown that with a dual loop configuration, the settling time of the loop can be made less than two symbol durations.

In Figure 2-3, the quantity $\frac{\eta_{RF}}{E_b/N_0}$ is plotted as a function of the number of symbols n_B in a burst for the different modulation schemes considered. For coherent PSK, $\frac{\eta_{RF}}{E_b/N_0}$ is given by

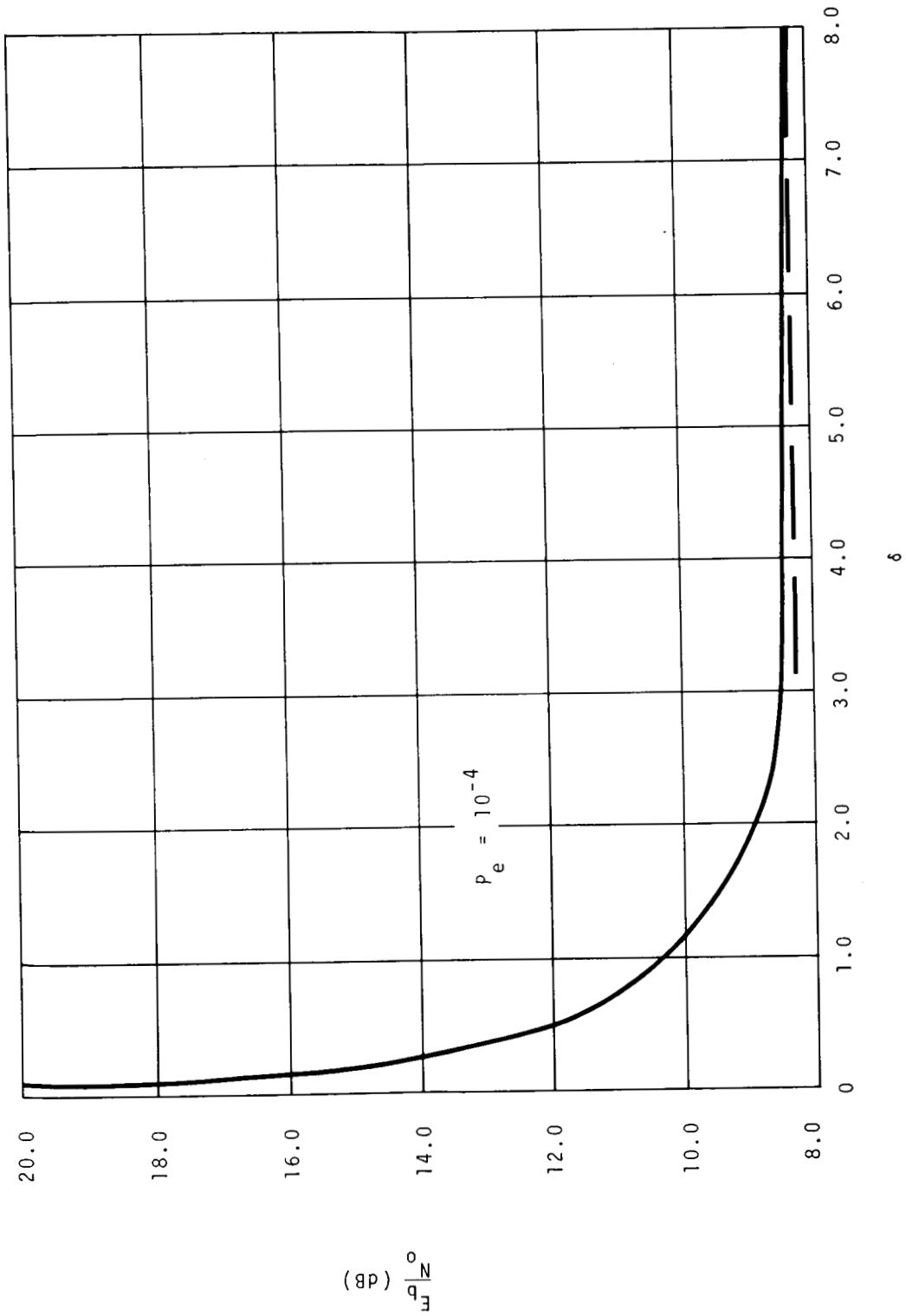


Figure 2-2. $\frac{E_b}{N_0}$ as a Function of δ for CPSK Modulation

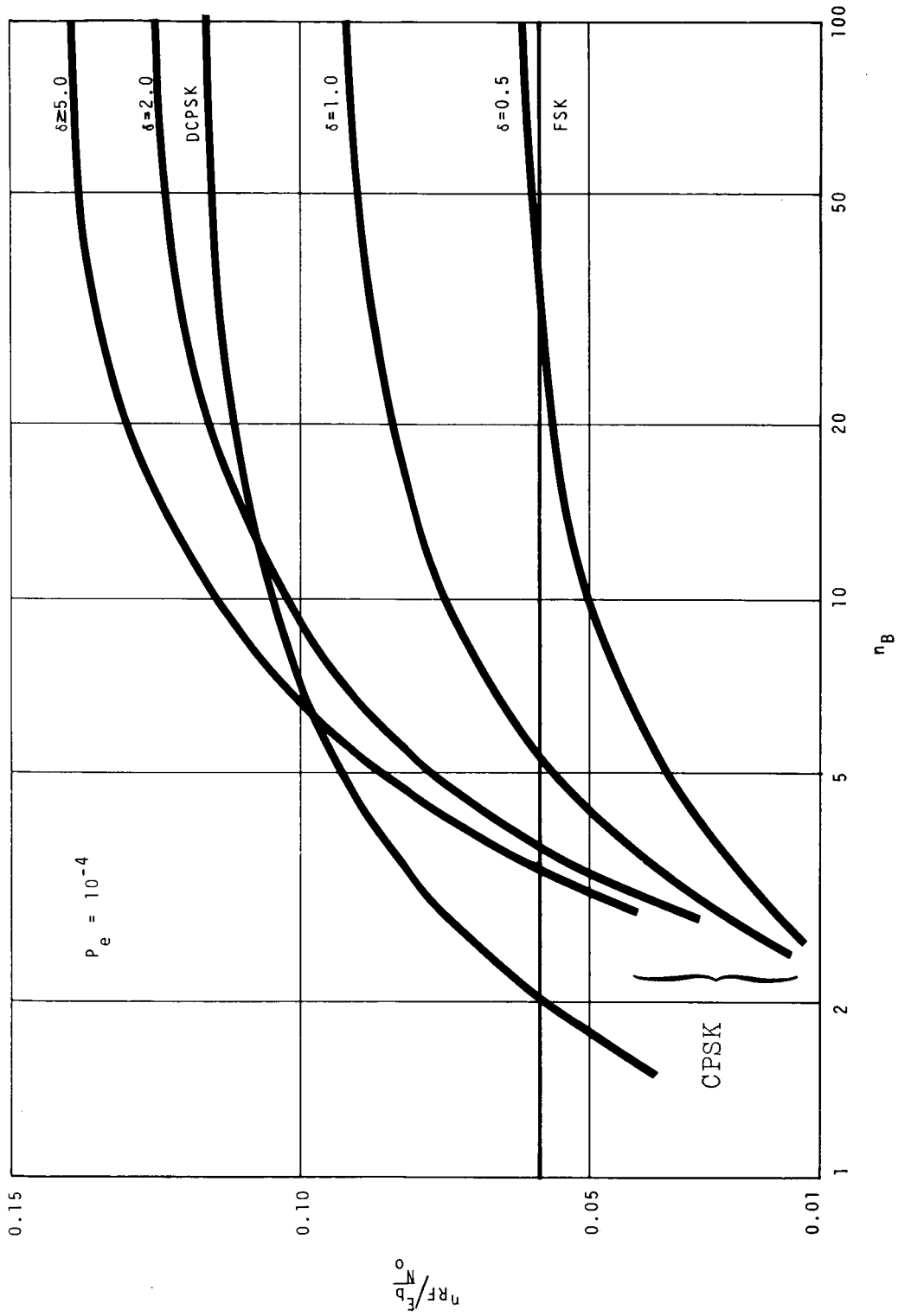


Figure 2-3. $\eta_{RF}/E_b/N_0$ Vs. Burst Length (n_B) for Various Modulation Techniques

$$\frac{\eta_{RF}}{E_b/N_o} = \frac{1 - 2/n_B}{\frac{E_b}{N_o}(\delta)} \quad (2-16)$$

where the relationship $\frac{E_b}{N_o}(\delta)$ versus δ , derived from Lindsey's data, is shown in Figure 2-2 for 10^{-4} error probability.

A variation of the coherent PSK system is the differentially coherent PSK system (DCPSK). In this system information is conveyed by the phase difference of the transmitted signal between adjacent signal elements. Thus, the absolute phase of the received signals is not required at the receiver. For this modulation scheme, the first symbol in the burst is used to establish phase; the remaining symbols use the immediately preceding symbol for a phase reference. Thus, for DCPSK, we get with $n_{RF} = 1$,

$$\frac{\eta_{RF}}{E_b/N_o} = \frac{1 - 1/n_B}{\frac{E_b}{N_o}} \quad (2-17)$$

which is also plotted in Figure 2-3 for direct comparison with CPSK. The value of E_b/N_o required for an error rate of 10^{-4} with DCPSK is 9.3 dB.

Differentially coherent phase shift keying is sometimes discarded because of the propensity for adjacent errors to occur. However, these double errors do not occur at all times. That is, the probability of error in the $(j + 1)$ -th bit, on the hypothesis that an error occurs on the j -th bit, is not unity.

A theoretical derivation (Reference 3) obtains a conditional probability of a double error, given a single error, of approximately 0.17 at an E_b/N_o of 9.3 dB for additive Gaussian noise. Further, Reference 3 shows an experimental value of 0.06 for the same E_b/N_o . Thus, the occurrence of double errors is not a major problem in DCPSK systems at the E_b/N_o normally used.

Digital differential detection (or differentially coded PSK) is sometimes employed in a CPSK system to resolve the 180° phase ambiguity. In this type system the conditional probability of the second error given the first error is essentially unity. Thus, any error correcting codes employed must provide for the correction of adjacent errors.

A noncoherent form of modulation such as noncoherent FSK is easy to implement and, being noncoherent, does not require the establishment of carrier phase and frequency, assuming that the rate of change of Doppler is small compared to the data rate. It will be assumed that the Doppler rate is negligible compared to the data rates of interest. (See Appendix A.)

For noncoherent FSK, $\eta_{RF} = 1$ since no symbols are required for RF synchronization.

Thus:

$$\frac{\eta_{RF}}{E_b/N_o} = \frac{1}{E_b/N_o} \quad (2-18)$$

which is independent of n_B . The performance of noncoherent FSK is also plotted in Figure 2-3. It is inferior to both CPSK and DCPSK modulation schemes for large n_B .

2.4.2 Bit Synchronization

In this paragraph, optimization of $\eta_{BS} \cos^2 \theta$ contained in Equation (2-11) will be considered for different synchronization techniques. The factor, η_{BS} , is the bit synchronization efficiency and accounts for the fraction of time during a frame interval devoted to bit synchronization. If m symbols are used for bit synchronization in every frame of n symbols, the bit sync efficiency can be conveniently represented by

$$\eta_{BS} = 1 - \frac{m}{n} \quad (2-19)$$

The phase jitter, θ , on the output of a bit synchronizer, is a random variable which can be approximated by a Gaussian distribution:

$$p(\theta) = \frac{\exp \left[-\theta^2 / 2\sigma_\theta^2 \right]}{\sqrt{2\pi\sigma_\theta^2}} \quad (2-20)$$

with zero mean and variance σ_θ^2 . Thus, the expected value of $\eta_{BS} \cdot \cos^2\theta$ is given by the first moment,

$$\overline{\eta_{BS} \cos^2\theta} = \left(1 - \frac{m}{n}\right) \int_{-\infty}^{\infty} \cos^2\theta \cdot p(\theta) d\theta \quad (2-21)$$

The integration can be easily performed, and we obtain

$$\overline{\eta_{BS} \cos^2\theta} = \left(1 - \frac{m}{n}\right) \left[\frac{1 + e^{-2\sigma_\theta^2}}{2} \right] \quad (2-22)$$

The expected value of $\eta_{BS} \cos^2\theta$ can be determined using Equation (2-22) for both bit coherent and noncoherent synchronization techniques.

2.4.2.1 Bit Coherent Synchronization

In most bit synchronization techniques, where the input signals are perturbed by noise, the local clock is derived from the data using a bit synchronizer, which is a form of phase-lock loop that locks on the baseband data. In a bit coherent system, the data clocks for all transmissions are coherent or synchronized. The local clock is derived from the frame synchronization symbols at the beginning of each frame. The resulting clock is maintained throughout the remainder of the frame and is employed to demodulate the data in all bursts. There will be a phase error θ between the clock and the data bursts due to errors in deriving the clock

and errors in the positioning of the bursts. Errors due to burst positioning are discussed in Paragraph 2.4.3; errors in deriving the clock are discussed in the following paragraphs. Obviously, if the burst positioning errors are large compared to a symbol duration, bit coherent synchronization cannot be used.

First, a sequence of m symbols in the frame sync is used to establish the phase of a local clock using a phase-locked loop. At the end of this sequence, provided the steady-state condition of the loop is reached, the variance of the phase error is (Reference 4):

$$\sigma_{\theta_0}^2 = \frac{1}{2 S/N} \text{ (radians)}^2 \quad (2-23)$$

where S/N is the signal-to-noise ratio in the loop bandwidth. A settling time of the loop of twice the reciprocal of the noise bandwidth is adequate if the initial phase error is less than about $\pi/4$ radians. The noise power is then:

$$N = N_0 B_L = \frac{2 N_0}{m T_B} \quad (2-24)$$

and

$$\sigma_{\theta_0}^2 = \frac{1}{m E_b / N_0} \quad (2-25)$$

for $E_b = S \cdot T_B =$ signal energy per bit.

After the end of the synchronizing symbols, an additional phase error will accumulate due to frequency errors. The total worst case error occurs at the end of the frame just before the beginning of the next sequence. For a frame length of n symbols (excluding the frame sync and guard band) of duration $T_F = \frac{2\pi n}{\omega_b}$, the worst case error is

$$\theta = \theta_0 + 2\pi \frac{\omega_0}{\omega_b} (n - m) \quad (2-26)$$

where ω_o is the frequency error. The total variance assuming independence between the two terms is

$$\sigma_{\theta}^2 = \sigma_{\theta_o}^2 + \sigma_{\omega}^2 (n - m)^2 \quad (2-27)$$

where

$$\sigma_{\omega}^2 = \left(2\pi \frac{\omega_o}{\omega_b}\right)^2 \quad (2-28)$$

It is assumed that both errors have a mean of zero so that the variance is identical to the second moment.

The clock frequency may be stored between the successive frames in several ways. Two of these will be considered.

2.4.2.1.1 Instantaneous Frequency Storage

At the end of the group of synchronizing symbols, the VCO voltage is clamped so that the last frequency is, in effect, stored on the VCO. If the phase noise of the VCO itself is kept small, then the frequency error is that due to the instantaneous frequency fluctuations caused by the input noise. The spectral density of the instantaneous frequency noise caused by a white additive Gaussian noise is also Gaussian. Its spectral density rises with the square of frequency and is ultimately limited by the bandpass filter that preceded the loop, in cascade with the closed loop system function. The minimum variance that can be obtained is (Reference 5):

$$\sigma_{\omega}^2 = \frac{N_o}{S} \frac{1}{4 \sqrt{2}} \left[\frac{2 \sqrt{2}}{3} B_L \right]^3 \quad (2-29)$$

where B_L is the noise bandwidth.

The angular frequency variance can be written in terms of the phase variance with the aid of Equations (2-24) and (2-25) as

$$\sigma_w^2 = \sigma_{\theta_0}^2 \frac{1.19}{(m T_b)^2} \quad (2-30)$$

Thus, using Equations (2-27) and (2-30) the variance of the phase error is

$$\sigma_{\theta}^2 = \frac{1}{m E_b/N_0} \left[1 + 1.19 \frac{(n - m)^2}{m^2} \right] \quad (2-31)$$

The expected value of $\eta_{BS} \cos^2 \theta$, given in Equation (2-22), can now be evaluated with the help of Equation (2-31). A graph of Equation (2-22) as a function of m/n is shown in Figure 2-4 for selected values of $m E_b/N_0$. The curves indicate a maximum of $(\eta_{BS} \cos^2 \theta)$ for certain combinations of m , n , and E_b/N_0 . To determine the maximum $(\eta_{BS} \cos^2 \theta)$ for a given value of n and E_b/N_0 , it is convenient to substitute x for m/n , in Equations (2-22) and (2-31). Thus, we obtain

$$\overline{\eta_{BS} \cos^2 \theta} = (1 - x) \left[\frac{1 + e^{-2\sigma_{\theta}^2}}{2} \right] \quad (2-32)$$

and

$$\sigma_{\theta}^2 = \frac{1}{n x E_b/N_0} \left[1 + 1.19 \frac{(1 - x)^2}{x^2} \right] \quad (2-33)$$

Taking the partial derivative of $\eta_{BS} \cos^2 \theta$ with respect to x and equating to zero, we get (with the approximation $\sigma_{\theta}^2 \ll 0.5$)

$$n E_b/N_0 x^2 = (3 - 2x) \left[1 + 1.19 \left(\frac{1 - x}{x} \right)^2 \right] - 2 \quad (2-34)$$

A general solution of Equation (2-34) is rather involved. However, it can be simplified for the range of interest $0.01 < x < 0.15$, i.e., $0.99 > \eta_{BS} > 0.85$, and we obtain:

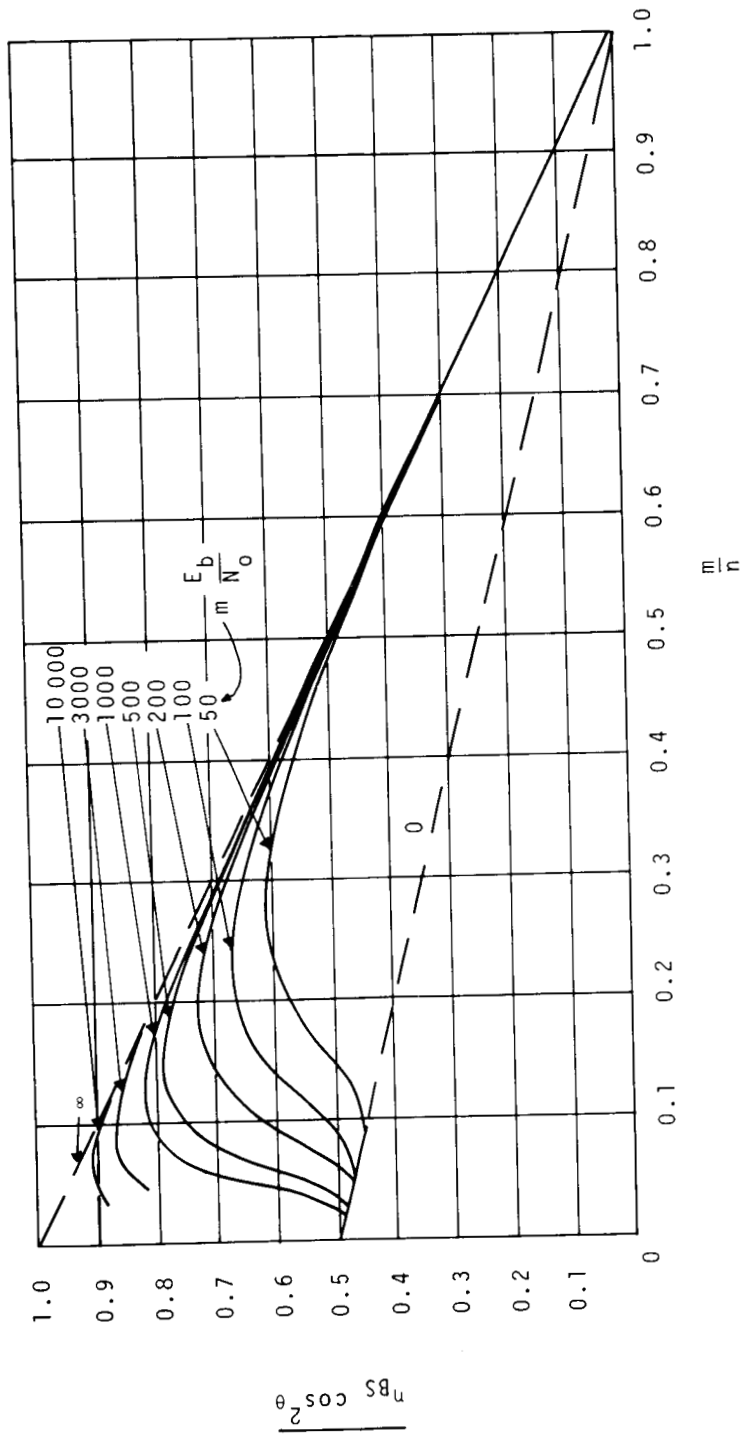


Figure 2-4. Expected Value of $\eta_{BS} \cos^2 \theta$ as a Function of $\frac{m}{n}$ for Instantaneous Frequency Storage Bit Coherent Synchronization

$$n E_b/N_o x^2 \approx 3.57 \frac{(1-x)^2}{x^2} \quad (2-35)$$

which has the general solution

$$x_{opt} = \frac{1}{2} \sqrt{\frac{3.57}{n E_b/N_o}} \left[-1 + \sqrt{1 + 4 \sqrt{\frac{n E_b/N_o}{3.57}}} \right] \quad (2-36)$$

In Figure 2-5 graphs of x_{opt} as a function of frame length n are shown for various values of E_b/N_o . Substituting the value of x from Equation (2-36) into Equation (2-32) gives the maximum of $(\eta_{BS} \cos^2 \theta)$ for a given value of n and E_b/N_o . This is plotted in Figure 2-6.

2.4.2.1.2 Average Frequency Storage

Under conditions of low Doppler and a stable clock source, the data rate varies slowly and an average instead of an instantaneous voltage can be clamped on the VCO between groups of synchronizing symbols. In the case of near-synchronous orbits the time interval that is available for averaging becomes quite large so that the frequency errors are then determined primarily by the stability of the frequency source and the VCO. If a crystal VCO is employed, a stability of one part in 10^6 to 10^8 is reasonable. Using a clock frequency at half the symbol rate the second term of Equation (2-27) is:

$$\sigma_w^2 (n-m)^2 = s^2 \pi^2 (n-m)^2 \quad (2-37)$$

for relative frequency stability, s . The worst case variance of the phase error is then

$$\sigma_\theta^2 = \frac{1}{m E_b/N_o} + s^2 \pi^2 (n-m)^2 \quad (2-38)$$

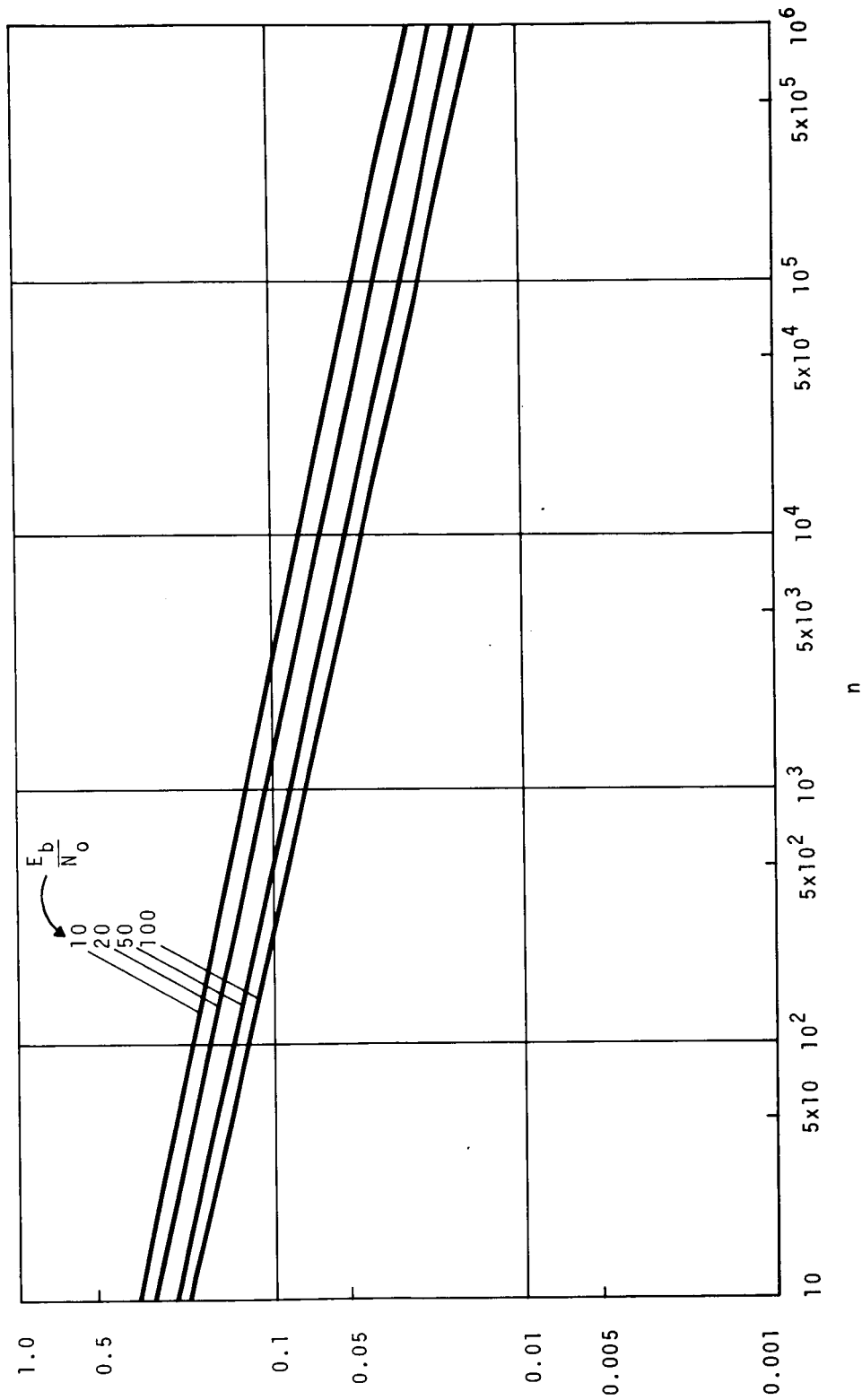


Figure 2-5. X_{opt} as a Function of Frame Length n for Instantaneous Frequency Storage Bit Coherent Synchronization

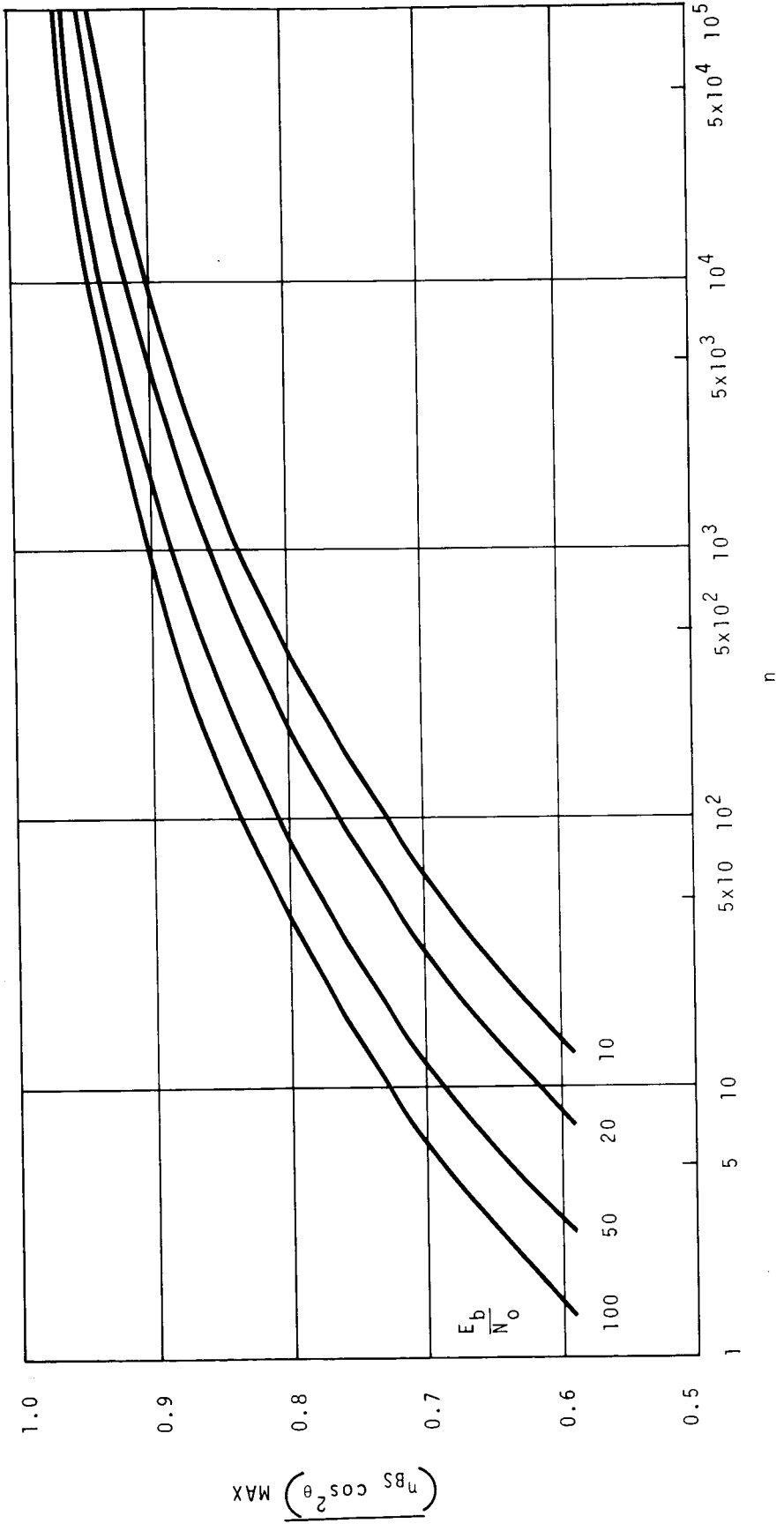


Figure 2-6. Maximum Expected Value of $\eta_{BS} \cos^2 \theta$ as a Function of Frame Length n for Instantaneous Frequency Storage Bit Coherent Synchronization

or with $x = m/n$,

$$\sigma_{\theta}^2 = \frac{1}{nx \frac{E_b}{N_0}} + s^2 \pi^2 n^2 (1 - x)^2 \quad (2-39)$$

To determine the maximum of $(\eta_{BS} \cos^2 \theta)$ for a known value of n , s , and E_b/N_0 we take the partial derivative of Equation (2-22) with respect to x and set it equal to zero. With the assumption $\sigma_{\theta}^2 \ll 0.5$, we obtain:

$$s^2 \pi^2 n^2 (1 - x)^2 + \frac{1 - 2x}{x^2} \cdot \frac{1}{n \frac{E_b}{N_0}} = 1 \quad (2-40)$$

For $x \ll 1$, $(1 - x)^2 \approx 1 - 2x$ and the preceding equation can be further simplified:

$$x^3 + \frac{(1 - s^2 \pi^2 n^2)}{2} x^2 - \frac{1}{2n \frac{E_b}{N_0}} = 0 \quad (2-41)$$

In a practical system, $s^2 \pi^2 n^2 \ll 1$, to keep the phase jitter small. If we now confine x to the region $0.01 < x < 0.15$ we can neglect x^3 in Equation (2-41) and get the approximate solution

$$x_{opt} = \frac{1}{\sqrt{n \frac{E_b}{N_0} (1 - s^2 \pi^2 n^2)}} \quad (2-42)$$

Graphs of x_{opt} as a function of n , for various values of s and E_b/N_0 , are shown in Figure 2-7. For a given s , the region in which the phase jitter is less than 0.1 is indicated. This is the region of practical interest and is the region for which x_{opt} was derived. By increasing the stability of the clock, the region of low phase jitter can be extended to higher values of n . The maximum value of $(\eta_{BS} \cos^2 \theta)$ can be determined by substituting x_{opt} into Equation (2-22). Plots of $(\eta_{BS} \cos^2 \theta)_{max}$ as a function of n are shown in Figure 2-8 for different values of s and E_b/N_0 .

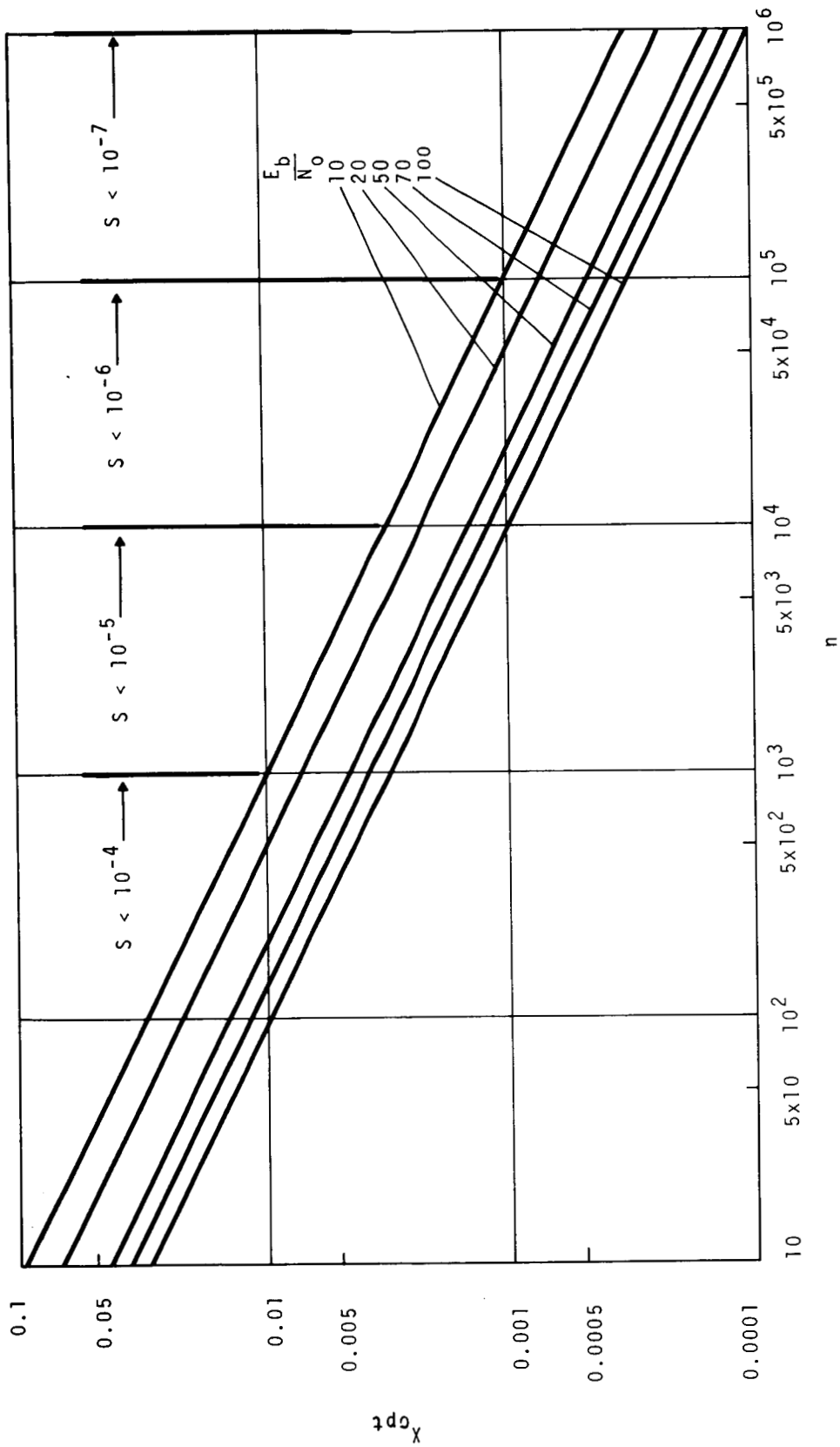


Figure 2-7. X_{opt} as a Function of Frame Length n for Average Frequency Storage Bit Coherent Synchronization

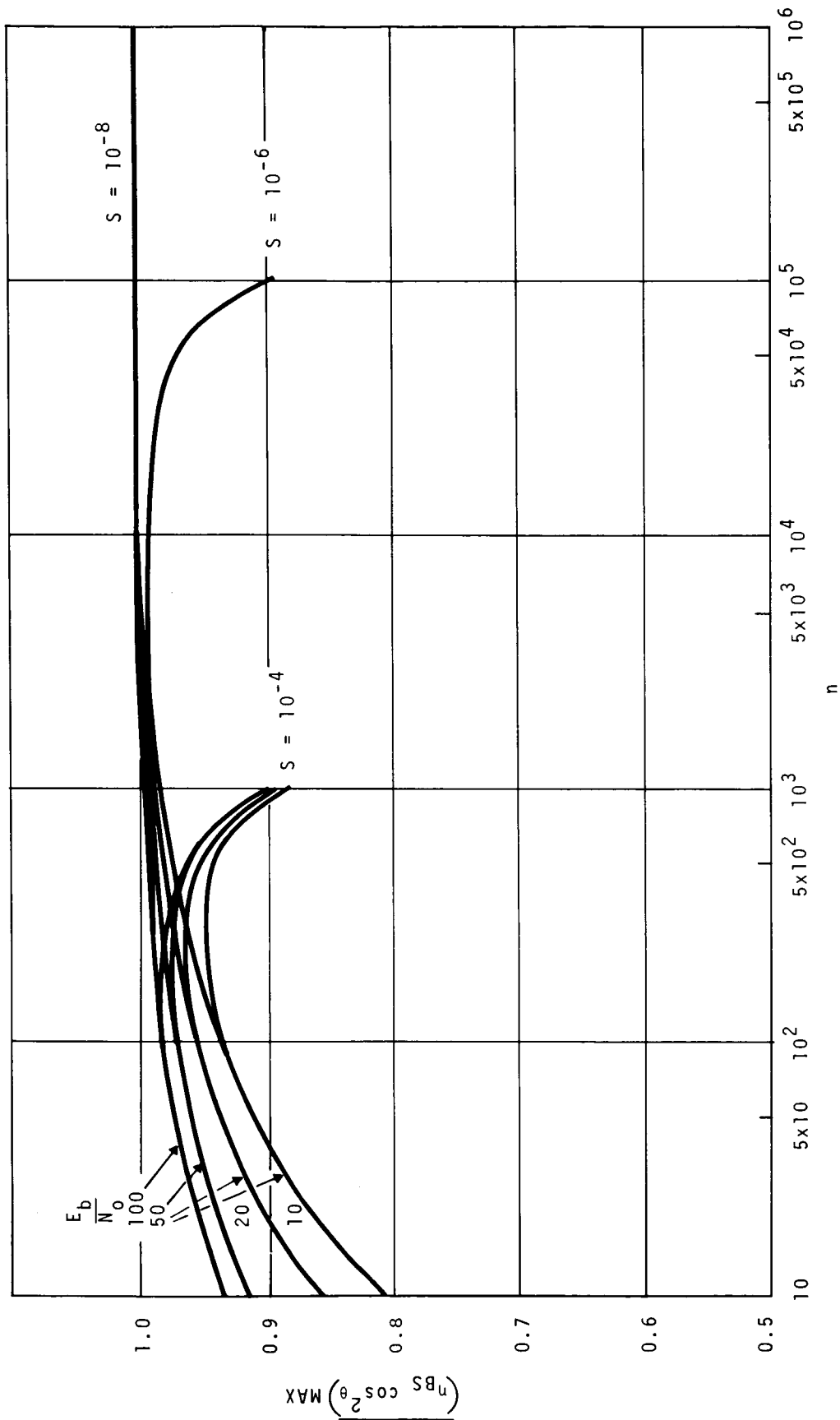


Figure 2-8. Maximum Expected Value of $\eta_{BS} \cos^2 \theta$ as a Function of Frame Length n for Average Frequency Storage Bit Coherent Synchronization

2.4.2.2 Bit Noncoherent Synchronization

In a bit noncoherent system, each burst is independently clocked and a local clock can be derived from synchronization symbols at the beginning of each burst. This system would be employed when the phase jitter due to the burst position system is large compared to the symbol duration and hence, bit coherence can not be maintained from burst to burst.

If the bit synchronizer requires m_B symbols each burst to derive the local clock, the variance of the phase error is given by Equation (2-25),

$$\sigma_\theta^2 = \frac{1}{m_B E_b/N_0} \quad (2-43)$$

This is the phase jitter after the m_B synchronization symbols and represents the worst case since the bit synchronizer would continue to operate during the remainder of the burst and further reduce the error. For a noncoherent system the expected value of $(\eta_{BS} \cos^2 \theta)$ is given by:

$$\overline{\eta_{BS} \cos^2 \theta} = \left(1 - \frac{m_B}{n_B}\right) \left[\frac{1 + e^{-2\sigma_\theta^2}}{2} \right] \quad (2-44)$$

The maximum value of $\overline{\eta_{BS} \cos^2 \theta}$ can be determined in a way analogous to the preceding sections. With $x_B = m_B/n_B$ and $\sigma_\theta^2 \ll 0.5$ we obtain the exact solution

$$x_{B_{opt}} = \frac{-1 + \sqrt{1 + n_B E_b/N_0}}{n_B E_b/N_0} \quad (2-45)$$

In Figure 2-9, $x_{B_{opt}}$ is plotted as a function of the burst length n_B , for different values of E_b/N_0 . The maximum value of $\overline{\eta_{BS} \cos^2 \theta}$ is obtained by substituting Equation (2-45) in Equation

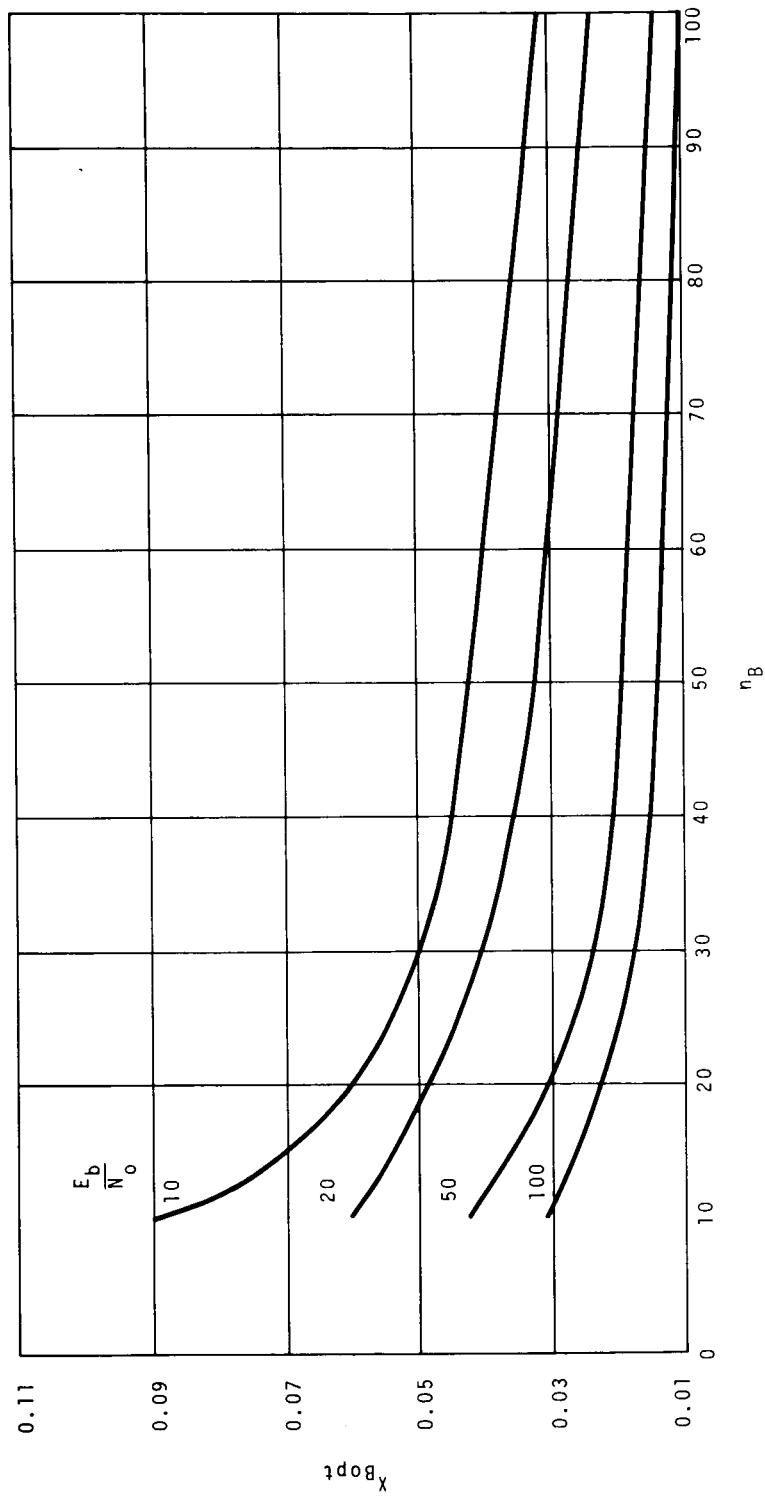


Figure 2-9. X_{Bopt} as a Function of Burst Length n_B for Bit Non-Coherent Synchronization

(2-44). A graph of $(\eta_{BS} \cos^2 \theta)_{\max}$ as a function of n_B is given in Figure 2-10.

2.4.3 Frame Synchronization

The frame efficiency, η_F , accounts for the fraction of total frame time devoted to framing and burst synchronization. From Equation (2-3)

$$\eta_F = 1 - \frac{T_{FS}}{T_F} - \frac{T_G}{T_F} \quad (2-46)$$

which may also be represented as:

$$\eta_F = 1 - \frac{n_{FS}}{n} - \frac{n_G}{n} \quad (2-47)$$

where n = Total number of symbols in a frame

n_{FS} = Total number of symbols devoted for frame synchronization

n_G = Total number of symbols used for guard bands

To increase the frame efficiency it is essential to reduce the number of frame synchronization symbols to a small fraction of the frame length, n , and minimize the guard bands between bursts. The frame lengths being considered in this study are on the order of a thousand bits or more (6 data bits/burst plus 1 guard bit for each of 200 accesses). The IRIG PCM telemetry standard uses a 31-bit word for synch with a maximum frame length of 2048 bits for an efficiency of 98.5 percent. Certain characteristics of a TDA system such as knowledge of the burst length and the existence of the guard bands can be used to improve the synch performance. Therefore, degradation in the frame efficiency, η_F , due to the presence of frame synch symbols can be made small and it will be neglected.

In a bit coherent system, the guard band between each burst must be an integral number of symbols. Thus, the minimum value of n_G , is $(N + 1)$ symbols for N bursts. To realize this minimum value for n_G , the errors in the burst position system must be much less than one symbol.

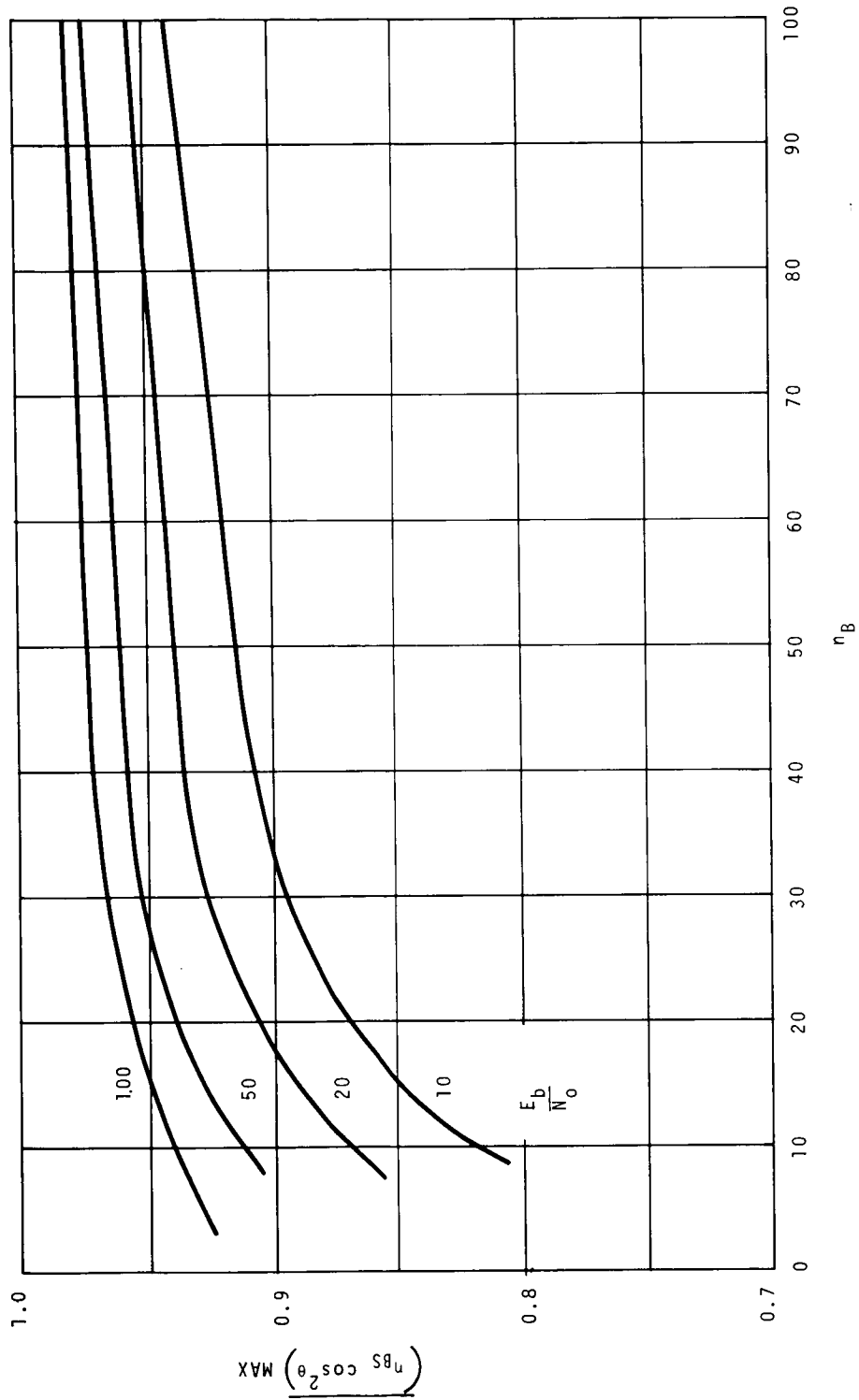


Figure 2-10. Maximum Expected Value of $\eta_{BS} \cos^2 \theta$ as a Function of Burst Length n_B for Bit Noncoherent Synchronization

2.4.3.1 Burst Position Errors

The burst position errors can be separated into the deterministic errors of a servo system and the statistical errors caused by noise in the input signals. To describe the burst position errors a particular frame organization is used. A master station transmits a frame sync code at the beginning of the frame; the remainder of the frame is devoted to N time slots. Station k derives a local reference clock from the frame sync and uses it to measure the time of occurrence of events received.

To position its own burst, station k measures the time of occurrence of the frame sync and the time of occurrence of its own burst. The result is compared with the desired time of arrival and the difference used to correct the transmission time and reduce the error. Thus, time at a slave station can be described as shown in Figure 2-11.

Considering zero time as the measured time of occurrence of the frame sync, the points in time that are of interest are:

$t_0 \triangleq$ Actual time of occurrence of the frame sync

$t_0' \triangleq$ Measured time of occurrence of the frame sync at the k-th station

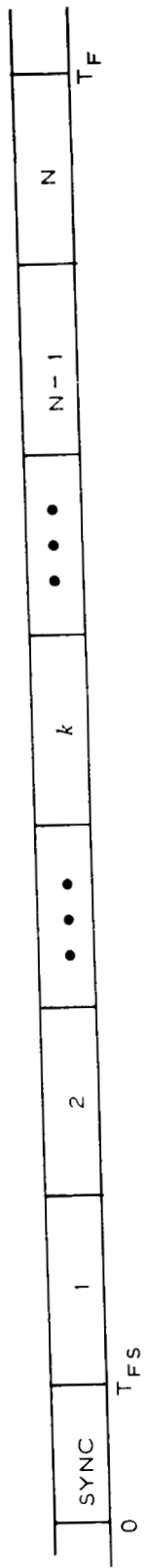
$t_k \triangleq$ The desired time of occurrence (of the k-th burst) according to an ideal clock

$t_k' \triangleq$ The desired time of occurrence according to the local reference clock at the k-th station

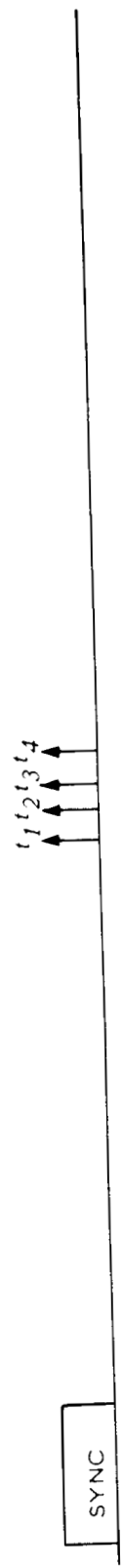
$t_m \triangleq$ Actual time of occurrence according to the ideal clock

$t_m' \triangleq$ Measured time of occurrence using the local clock

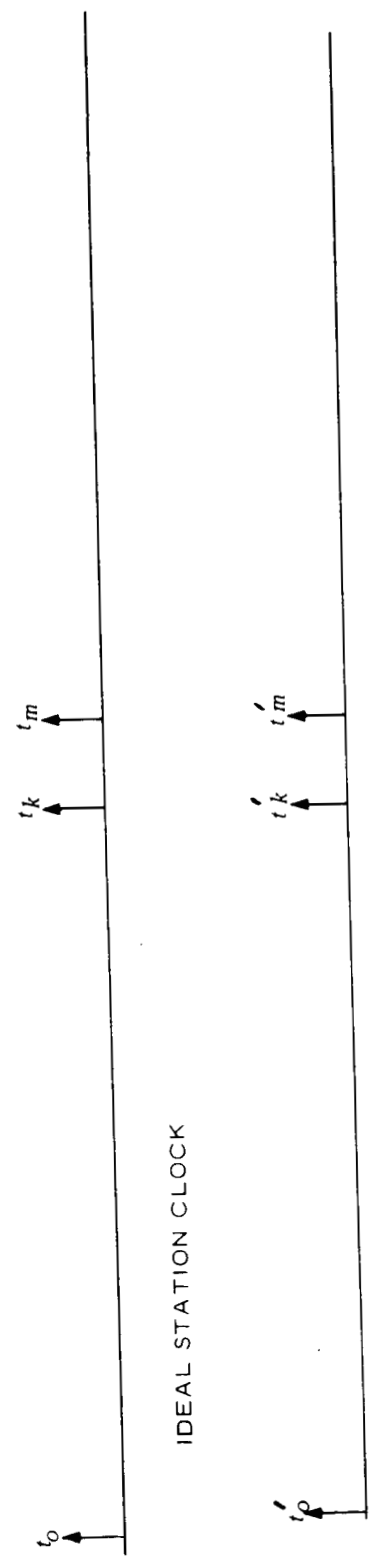
The burst position error consists of several terms. The first error $t_k' - t_k$ includes a measurement error ϵ_{ms} of the time of occurrence of the frame sync and a translation error ϵ_t due to any frequency error in the local reference clock. Thus,



(a) FRAME AT MASTER STATION



(b) FRAME AT *k*th STATION



IDEAL STATION CLOCK

(c) *k*th STATION CLOCK

Figure 2-11. Timing Diagram

$t_k' - t_k = \epsilon_{ms} + \epsilon_t$. The error $t_m' - t_k$ is the measurement error of the time of arrival of the k-th signal, ϵ_{ks} , plus the burst position error according to the local clock. The actual error signal should be $t_m - t_k$ but the one measured is

$$t_k' - t_m' = t_k - t_m + (\epsilon_{ms} + \epsilon_{ks} + \epsilon_t) \quad (2-48)$$

The three errors are independent random variables with zero mean. The remaining error is the deterministic error ϵ_b of the servo loop.

The servo loop will have a time constant which in effect averages the measurement errors. If the time constant is equal to P periods, the total burst position error can be represented by:

$$\epsilon_T = \epsilon_b + \text{p.f.} \left[\frac{1}{P} (\sigma_{ms}^2 + \sigma_{ks}^2 + \sigma_t^2) \right]^{\frac{1}{2}} \quad (2-49)$$

where σ represents the standard deviation of each random variable and p.f. is the peak factor that is desired, (i.e., the number of standard deviations required for an adequate margin; for example, p.f. = 3 results in a probability of 2×10^{-5} that the margin will be exceeded).

The same errors occur at a third station that is to receive the transmission from station k. This receiving station must also generate a local reference clock from the frame synchronization. This local reference clock will have a phase error with respect to the k-th burst in addition to the burst position error. This error can be described by a measurement error and translation error such as that of $t_k' - t_k$ of the k-th station.

2.4.3.2 Burst Synchronization System

The mathematical model for the burst synchronization system is shown in Figure 2-12. The desired value of delay, τ_i , to achieve perfect placement of the burst in its assigned time slot

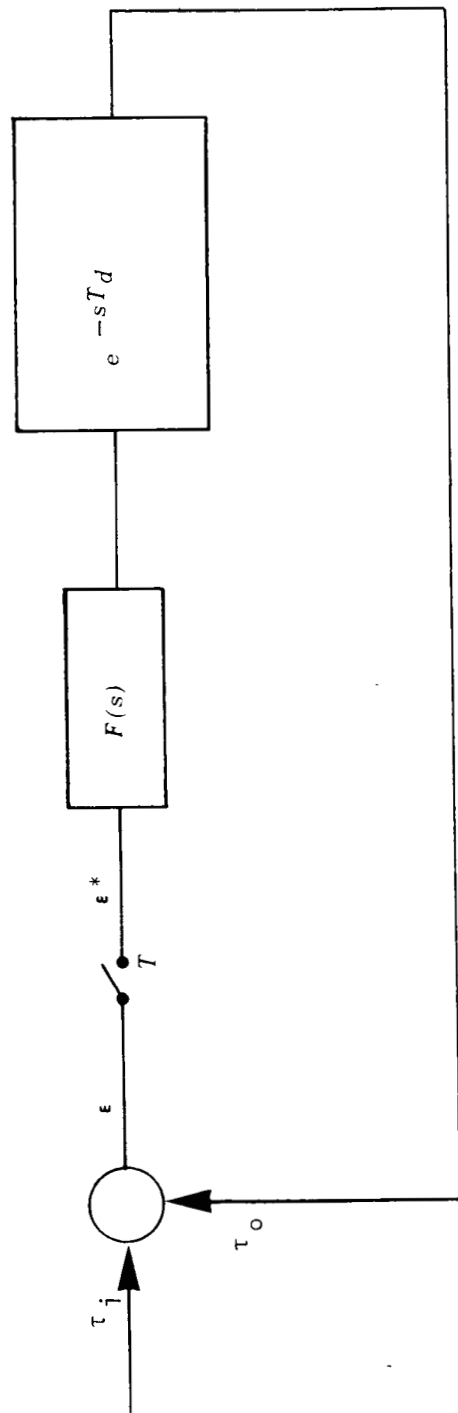


Figure 2-12. Burst Synchronization System

is compared with the actual value of delay, τ_o , to generate the delay error, ϵ . This error is, however, observed only at intervals (once every frame for each burst) of period T , which may be set equal to the frame interval T_F . This is represented in the figure by a sampling switch. The sampled error at its output ϵ^* is operated on by a filter, which has a second order transfer function of the form

$$F(s) = \frac{K_2}{s^2} (1 + T_1 s) \quad (2-50)$$

The effect of the transfer function $F(s)$ is to control the delay in the system. However, its effect is not felt until a later time because of the inherent propagation delay T_d . This is represented in Figure 2-12 by e^{-sT_d} . The propagation delay can be expressed as $n + \lambda$ periods of T , or

$$\frac{T_d}{T} = n + \lambda \quad (2-51)$$

where n is an integer and λ lies between zero and one. Because of the sampled data nature of the system, it is convenient to use the z -transform method of analysis. A modified open loop z transform of a second order system of Equation (2-50) is given by:

$$G(z) = K_2 \frac{T + [T_1 + (1 - \lambda)T] (z - 1)}{z^n (z - 1)^2} \quad (2-52)$$

2.4.3.2.1 Stability

The system will be unstable if the characteristic equation

$$1 + G(z) = 0 \quad (2-53)$$

has any root outside the unit circle. In this case

$$K_2 \left\{ T + \left[T_1 + (1 - \lambda)T \right] (z - 1) \right\} + z^n (z - 1)^2 = 0 \quad (2-54)$$

is the characteristic equation. If the integer n is greater than one, the process of extracting roots becomes extremely involved. Another approach to determine the stability of the system is to replace z by $e^{j\omega T}$ and examine the behavior of $G(e^{j\omega T})$ as ω varies. Thus, the gain and phase of the modified open loop function $G(e^{j\omega T})$ is found to be:

$$|G(e^{j\omega T})| = \frac{T \cdot K_2}{4 \sin \frac{\omega T}{2}} \left[\left(2 \frac{T_1}{T} - 2\lambda + 1 \right)^2 + \cot^2 \frac{\omega T}{2} \right]^{\frac{1}{2}} \quad (2-55)$$

and

$$\phi = -\frac{\pi}{2} - (n + \frac{1}{2}) \omega T - \tan^{-1} \frac{\cot \omega T / 2}{\left(2 \frac{T_1}{T} - 2\lambda + 1 \right)} \quad (2-56)$$

The system is unconditionally unstable if the gain is unity when the phase is 180° . To simplify the preceding expressions, the following approximations are made which are valid for virtually all conditions of interest:

$$\frac{\omega T}{2} \ll 1$$

and

$$(R + 1) \gg \frac{\omega T}{2}$$

where $R = 2\left(\frac{T_1}{T} - \lambda\right)$

Incorporation of the preceding approximations into Equation (2-56) yields

$$\phi = -\frac{\pi}{2} - (2n + 1) \frac{\omega T}{2} - \frac{2}{\omega T} \frac{1}{(R + 1)} \quad (2-57)$$

which can be maximized to obtain:

$$\left(\frac{\omega T}{2}\right)_{\text{opt}}^2 = \frac{1}{(R + 1)(2n + 1)} \quad (2-58)$$

Substituting Equation (2-58) into Equation (2-57) gives the maximum phase

$$\phi_{\text{max}} = -\frac{\pi}{2} - 2(2n + 1)\left(\frac{\omega T}{2}\right)_{\text{opt}} \quad (2-59)$$

which, for ϕ_{max} equal to $-\pi$, yields

$$\left(\frac{\omega T}{2}\right)_{\text{opt}} = \frac{\pi}{4} \frac{1}{(2n + 1)} \quad (2-60)$$

Equations (2-58) and (2-60) determine the relationship between R and n

$$\frac{2n + 1}{R + 1} = \left(\frac{\pi}{4}\right)^2 \quad (2-61)$$

The magnitude of $G(e^{j\omega T})$ at this frequency will be less than unity if:

$$K_2 \text{ max} < \frac{4 \sin\left(\frac{\omega T}{2}\right)_{\text{opt}}}{T \left[(R + 1)^2 + \cot^2\left(\frac{\omega T}{2}\right)_{\text{opt}} \right]^{\frac{1}{2}}} \quad (2-62)$$

or with the approximations mentioned above

$$K_2 \text{ max} < \frac{4}{T} \cdot \left(\frac{\pi}{4}\right)^3 \cdot \frac{1}{(2n + 1)^2} \cdot \frac{1}{\left[1 + \left(\frac{\pi}{4}\right)^2\right]^{\frac{1}{2}}} \quad (2-63)$$

2.4.3.2.2 Margin

The preceding paragraphs were a discussion of the stability criterion of a second-order burst synchronization system and established a bound for the maximum allowable gain, when the phase equals 180° . In a practical system, it is customary to have some phase margin; i.e., to ensure that when the gain of the system is unity the phase is less than 180° . This will provide a margin against gain and phase variations in the system. A phase margin can be defined as:

$$M = - \frac{\pi}{\phi_{\max}} \quad (2-64)$$

or from Equation (2-59)

$$M = \frac{\pi}{\frac{\pi}{2} + 2(2n + 1)\left(\frac{\omega T}{2}\right)_{\text{opt}}} \quad (2-65)$$

Using, as an example, a conservative value for M of $4/3$, which corresponds to $\phi_{\max} = -\frac{3\pi}{4}$, we obtain from Equation (2-65)

$$\left(\frac{\omega T}{2}\right)_{\text{opt}} = \frac{\pi}{8} \frac{1}{(2n + 1)} \quad (2-66)$$

The relationship between R and n can be established from Equations (2-58) and (2-66):

$$\frac{2n + 1}{R + 1} = \left(\frac{\pi}{8}\right)^2 \quad (2-67)$$

Thus, Equations (2-66) and (2-67) describe the point at which the gain can be allowed to be unity, or from Equation (2-55)

$$K_2 = \frac{4}{T} \cdot \left(\frac{\pi}{8}\right)^3 \cdot \frac{1}{(2n + 1)^2} \cdot \left[1 + \left(\frac{\pi}{8}\right)^2\right]^{\frac{1}{2}} \quad (2-68)$$

In practice, the filter $F(S)$ will usually be preceded by a hold circuit, in which case the required gain of the filter is $K_2' = K_2/T$, where T is the hold time.

2.4.3.2.3 Burst Position Error

The steady-state error of the burst synchronization system at any sampling instant (mT) may be expressed by the error series (Reference 6)

$$\epsilon(mT) = c_0 \tau_d(mT) + c_1 \dot{\tau}_d(mT) + \frac{c_2}{2!} \ddot{\tau}_d(mT) + \frac{c_3}{3!} \tau_d^{(3)}(mT) + \dots \quad (2-69)$$

where the points indicate differentiation with respect to time and the error coefficients are given by the relation

$$c_k = \left. \frac{d^k W^*(s)}{ds^k} \right|_{s=0} \quad (2-70)$$

$W^*(s)$ is the system-error pulse-transfer function in terms of the starred transform which is obtained by the substitution $z = e^{Ts}$. The system-error pulse-transfer function in terms of z -transform is defined as

$$W(z) = \frac{1}{1 + G(z)} \quad (2-71)$$

from which the starred transform

$$W^*(s) = \frac{1}{1 + G(e^{Ts})} \quad (2-72)$$

can be easily obtained. Thus, for the burst synchronization system of Figure 2-12 $W^*(s)$ is given by

$$W^*(s) = \frac{e^{nTs} (e^{Ts} - 1)^2}{e^{nTs} (e^{Ts} - 1)^2 + K_2 \left\{ T + [T_1 + (1 - \lambda)T] (e^{Ts} - 1) \right\}} \quad (2-73)$$

The error coefficients c_k may be easily calculated from the preceding equation

$$\begin{aligned} c_0 &= W^*(0) = 0 \\ c_1 &= \left. \frac{dW^*}{ds} \right|_{s=0} = 0 \\ c_2 &= \left. \frac{d^2 W^*}{ds^2} \right|_{s=0} = 2 \frac{T}{K_2} \\ c_3 &= \left. \frac{d^3 W^*}{ds^3} \right|_{s=0} = 6 \frac{T}{K_2} [T_1 + (2 - \lambda - n)T] \end{aligned} \quad (2-74)$$

and the steady-state error at a sampling instant, mT , is

$$\epsilon(mT) = \frac{T}{K_2} \left[\ddot{\tau}_d(mT) + (T_1 + (2 - \lambda - n)T) \dddot{\tau}_d(mT) + \dots \right] \quad (2-75)$$

2.4.4 Sample Calculation

In the following, the deterministic burst position steady-state error for a synchronous satellite orbit will be calculated. When the eccentricity, e , is small the following approximate expression for $\tau_d(t)$ can be derived from (Reference 7):

$$\tau_d(t) = \frac{2a(1 - e^2)}{c} [1 - e \cos \omega t] - \frac{2R_e}{c} \quad (2-76)$$

where $a = 26180$ miles = Semimajor axis of satellite orbit

$\omega = 7.3 \times 10^{-5}$ radians/second = Angular velocity of the earth

$c = 186000$ miles/second = Speed of light

$R_e = 3960$ miles = Radius of earth

Thus, the steady-state error for a synchronous satellite orbit can be obtained by substituting $\ddot{\tau}_d$ and $\dddot{\tau}_d$ from Equation (2-76) into Equation (2-75):

$$\epsilon(mT) = \frac{T}{K_2} \cdot \frac{2ae(1 - e^2)}{c} \cdot \omega^2 \begin{bmatrix} \cos \omega mT - \omega[T_1 + (2 - \lambda - n)T] \\ \sin \omega mT \end{bmatrix} \quad (2-77)$$

At this point, let us calculate the maximum steady-state error, assuming an eccentricity of 0.01 and a sampling period of 10^{-3} seconds. The quantities necessary to evaluate Equation (2-77) can be obtained as follows:

$$\text{Round trip delay } T_d = 2 \frac{a - R_e}{c} = 0.24 \text{ second}$$

$$n = \frac{T_d}{T} = 240$$

For large values of n , Equation (2-67) and (2-68) can be simplified

$$T_1 \approx \left(\frac{8}{\pi}\right)^2 T_d = 1.56 \text{ seconds}$$

$$K_2' = \frac{K_2}{T} \approx \frac{1}{T_d^2} \frac{\left(\frac{\pi}{8}\right)^3}{\left[1 + \left(\frac{\pi}{8}\right)^2\right]^{\frac{1}{2}}} = \frac{1}{17.8 T_d^2} = 0.98 \text{ s}^{-2}$$

$$\text{and } T_1 + (2 - \lambda - n)T \approx T_1 - T_d = 1.32 \text{ seconds}$$

Since the product

$$\omega[T_1 + (2 - \lambda - n)T] \ll 1$$

for any reasonable sampling rate, the first term in Equation (2-77) is dominant, and the error is a sinusoid whose amplitude is

$$\epsilon_{\max} = 15.25 \times 10^{-12} \text{ seconds}$$

The burst synchronization system has a time constant, T_1 , which, in effect, averages the measurement errors. Thus, the variance of the statistical errors (with zero mean and a total standard deviation σ_m) will be reduced by

$$\sigma^2 = \frac{T}{T_1} \sigma_m^2 = \left(\frac{\pi}{8}\right)^2 \frac{T}{T_d} \sigma_m^2 = \frac{\sigma_m^2}{P}$$

where P is the reduction factor introduced in Equation (2-49). With $T_d = 0.24$ sec. and $T = 10^{-3}$ sec. we obtain

$$P = \left(\frac{8}{\pi}\right)^2 \frac{T_d}{T} = 1560$$

The statistical error consists of timing and measurement errors. In general, the measurement errors can be held to the order of 1 part in 10^8 in a system using synchronous satellites. Assuming a mean standard deviation of 10^{-8} seconds for the statistical errors and a peak factor of 3 to ensure adequate margin, the total burst position error can be calculated from Equation (2-49).

$$\epsilon_T = 15.25 \times 10^{-12} + \frac{3 \times 10^{-8}}{39} = 7.85 \times 10^{-10} \text{ sec.}$$

The total burst position error is therefore dominated by the measurement error and the deterministic error of the servo loop is negligible for this example.

Baseband data rates on the order of 30 to 50 kb/s are reasonable for small users while the burst data rates are many times higher, depending on the number of accesses. Assuming a maximum burst data rate of 10 Mb/s (equivalent to 200 50 kb/s users) the maximum burst position error is only

$$n = 7.85 \times 10^{-10} \times 10^7 = 0.0078 \text{ bits}$$

Since the burst position error can be made much less than a bit when a synchronous satellite is used in the system, bit coherent synchronization can be employed.

Because of the relatively modest system data rate of 10 Mb/s used in this numerical example, the distortion effects of propagation can be neglected. If a very large number of users were involved and/or if higher user data rates were necessary, these effects would have to be included.

SECTION 3

CONCLUSIONS

As stated in the introduction, the purpose of this study was to investigate the feasibility of Time Division Access (TDA) and develop an optimizing technique for small user access, satellite communication systems. For the small user system, the optimization philosophy was to maximize the number of accesses which can be obtained for a given received carrier to noise density ratio. This was shown to be equivalent to maximizing the system figure of merit

$$F = \frac{\eta_{RF}}{\frac{E_b}{N_0}(\delta)} \cdot \eta_{BS} \cos^2 \theta \cdot \eta_F$$

The analysis of each of the three terms in Paragraphs 2.4.1, 2.4.2, and 2.4.3 under the conditions of transmission stated in Section 2 leads to the following conclusions for binary TDA systems using synchronous satellites.

a. For burst lengths greater than 6 bits, coherent PSK modulation with a self-synchronizing demodulator employing an acquisition loop and carrier tracking loop is optimum.

b. A bit coherent synchronization system using average frequency storage is optimum for a wide variation in frame lengths (e.g., for a stability, $S = 10^{-6}$, $\eta_{BS} \cos^2 \theta$ is maximum for $1000 \leq n \leq 10,000$ bits) providing the burst position error can be held much below one bit duration.

c. A second order burst synchronizing system used with a stationary satellite will reduce the burst position jitter to a small fraction of a bit. Thus the required guard intervals need only be one bit.

To utilize the results of this study in a system synthesis, the nature and bounds of the small users requirements and the optimum voice digitization techniques must be determined. These two factors can then be used to develop the burst length and the frame

length constraints. The satellite and ground station parameters can be selected to result in feasible values for carrier to noise density ratio, C/kT , which will allow the postulation of candidate system configurations. Analysis of the user requirements, modified by current operational communication practices, will then lead to the development of potential system control philosophies.

REFERENCES

1. Lawton, J. G., Comparison of Binary Data Transmission Systems, Proc. 2nd Natl. Conf. Military Electron., 1958.
2. Lindsey, W. C., Phase-Shift-Keyed Signal Detection with Noisy Reference Signals, IEEE Trans. on Aerospace and Electronic Systems, July 1966.
3. Salz, J. and Saltzberg, B. R., Double Error Rates in Differentially Coherent Phase Systems, IEEE Trans. on Communication Systems, June 1964.
4. Viterbi, A. J., Phase-Lock-Loop Systems, Space Communications, Edited by A. V. Balakrishnan, McGraw-Hill Book Company, Inc. New York, 1963.
5. Martin, B. D., The Pioneer IV Lunar Probe: A Minimum Power FM/PM System Design, Jet Propulsion Laboratory Tech. Report No. 32-215.
6. Tou, J. T., Digital and Sampled-Data Control Systems, McGraw-Hill, New York, 1959.
7. Goldstein, H., Classical Mechanics, Addison-Wesley Publishing Co., Inc., Reading, Mass., 1959.
8. Van Trees, H. L., Optimum Power Division in Coherent Communication Systems, IEEE Trans. Space Electronics and Telemetry, March 1964.
9. Sanneman, R. W. and Rowbotham, J. R., Unlock Characteristics of the Optimum Type II Phase-Locked Loop, IEEE Trans. on Aerospace and Navigational Electronics, March 1964.

APPENDIX A

ANALYSIS OF PSK DEMODULATOR FOR TDA SYSTEMS

A.1 PSK DEMODULATION

The optimum binary communication technique in the presence of white Gaussian noise (i.e., that which produces the minimum error rate for a given E_b/N_0) is the coherent detection of binary antipodal or anticorrelated signals. The transmitted signals, $S_1(t)$ and $S_2(t)$ must satisfy the following relationships.

$$\int_0^{T_b} S_1(t) S_2(t) dt = -E_b$$
$$\int_0^{T_b} S_1^2(t) dt = \int_0^{T_b} S_2^2(t) dt = E_b$$

Binary phase shift keying (PSK) satisfies these relationships where:

$$S_1(t) = A \cos \omega_0 t$$
$$S_2(t) = A \cos (\omega_0 t + \pi) = -A \cos \omega_0 t = -S_1(t)$$
$$A = \sqrt{\frac{2E_b}{T_b}}$$

This appendix presents the analysis of a particular type of coherent receiver for use in TDA systems. This receiver has been assumed in the report.

In general, the communication channel imparts a random phase shift to the signal and adds Gaussian noise. A general model of the system is shown in Figure A-1a. The input to the modulator, $m(t)$, is a binary message with a bit duration of T_b :

$$m(t) = 1 \text{ or } 0, \quad t_0 + n T_b \leq t \leq t_0 + (n + 1) T_b$$

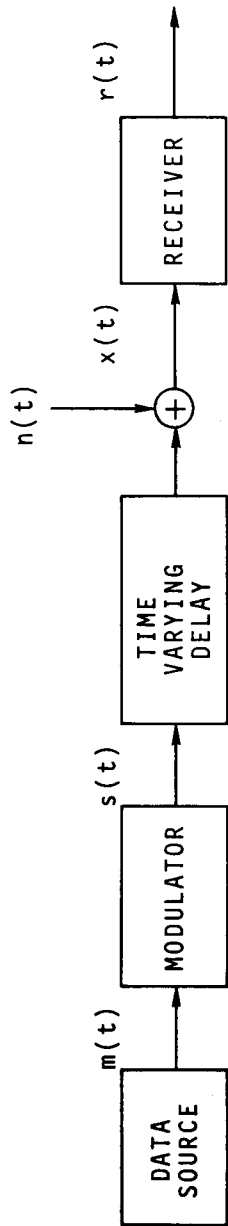


Figure A-la. Model of Communications Channel

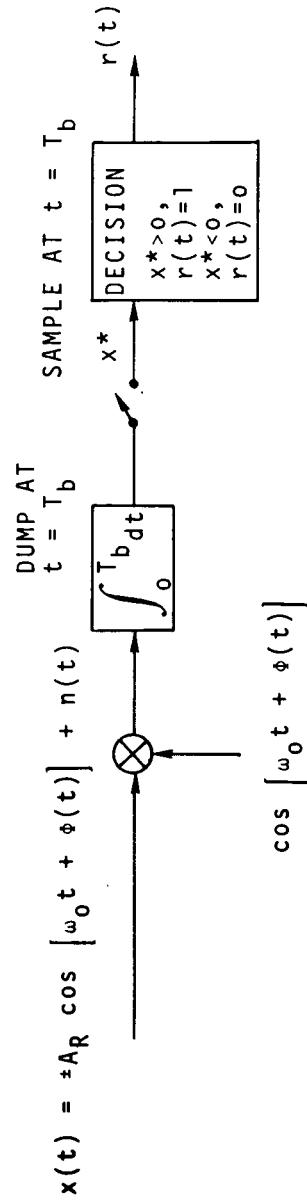


Figure A-lb. Model of Optimum PSK Receiver

The signal out of the modulator, $S(t)$, is a function of $m(t)$:

$$\begin{aligned} m(t) = 1 & \quad , S(t) = A \cos \omega_0 t \\ m(t) = 0 & \quad , S(t) = -A \cos \omega_0 t \end{aligned}$$

The non-fading Gaussian channel imparts a random phase shift, $\phi(t)$, to the signal and adds Gaussian noise, $n(t)$. Thus, the input to the receiver $X(t)$ is of the following form:

$$X(t) = \pm A_R \cos \left(\omega_0 t + \phi(t) \right) + n(t)$$

Figure A-1b shows the model of the optimum receiver for PSK signals imbedded in Gaussian noise. To coherently demodulate the received signal, a replica of the carrier with the random phase shift must be produced at the receiver.

In general, there are two methods of accomplishing this. The first method is to transmit an auxiliary signal (pilot tone or synchronous subcarrier) for the purpose of measuring the channel. The second method is to derive a reference carrier from the received, information-bearing signal, $X(t)$. These two methods were analyzed by Van Trees (Reference 8) and it was shown that a self-synchronizing technique, represented by the second method, results in the optimum utilization of power. Lindsey (Reference 2) has analyzed the performance of a self-synchronizing PSK demodulator which employs a squaring loop to derive a reference carrier from the PSK signal. The error rate performance of this demodulator is a function of the parameter, δ , defined as follows:

$$\delta = \frac{R}{B_L} \left[1 + \frac{N_0 W}{2S} \right]^{-1}$$

where:

- R = data rate
- B_L = single sided noise bandwidth of the phase-locked loop
- N_0 = single sided input noise spectral density
- S = input signal power
- W = bandwidth of the bandpass filter which precedes the squaring device

If the bandwidth of the bandpass filter is equal to twice the data rate and the input signal-to-noise ratio or energy-per-bit-to-noise density ratio ($E/N_0 = S/N_0R$) is large, δ may be approximated as follows:

$$\delta \approx \frac{R}{B_L}$$

The model of a receiver, based on the squaring loop, is shown in Figure A-2. The receiver has two tracking loops. Loop 1 is used for acquisition of the carrier and loop 2 tracks the carrier during data demodulation.

This receiver operates as follows. During the carrier sync portion of the burst, the symbols transmitted will be a sequence of binary ones, the switch in position A, and loop 1 operative. Since there is no modulation on the carrier, it can be tracked directly (i.e., squaring is not required). The loop bandwidth of the acquisition loop can be made large to lower the acquisition time, if necessary. After the carrier has been acquired in loop 1, loop 2 (the squaring loop which has narrower loop bandwidth) is switched in to reduce the phase jitter on the reference due to noise at the input. Thus, loop 1 must remove the initial frequency and phase error and loop 2 must further reduce the phase jitter. In addition, since initial acquisition was achieved without the squaring loop, the 180° ambiguity normally attendant to its use is removed.

The acquisition or lock-on time of a phase lock loop with a noise free input is a function of the loop parameters and the initial conditions (i.e., initial frequency and phase errors).

A.2 INITIAL CONDITIONS

The worst case initial phase error is π radians. The worst case initial frequency error occurs when a station is receiving two bursts from two different transmitting stations during a frame and must demodulate them with the same receiver. Referring to

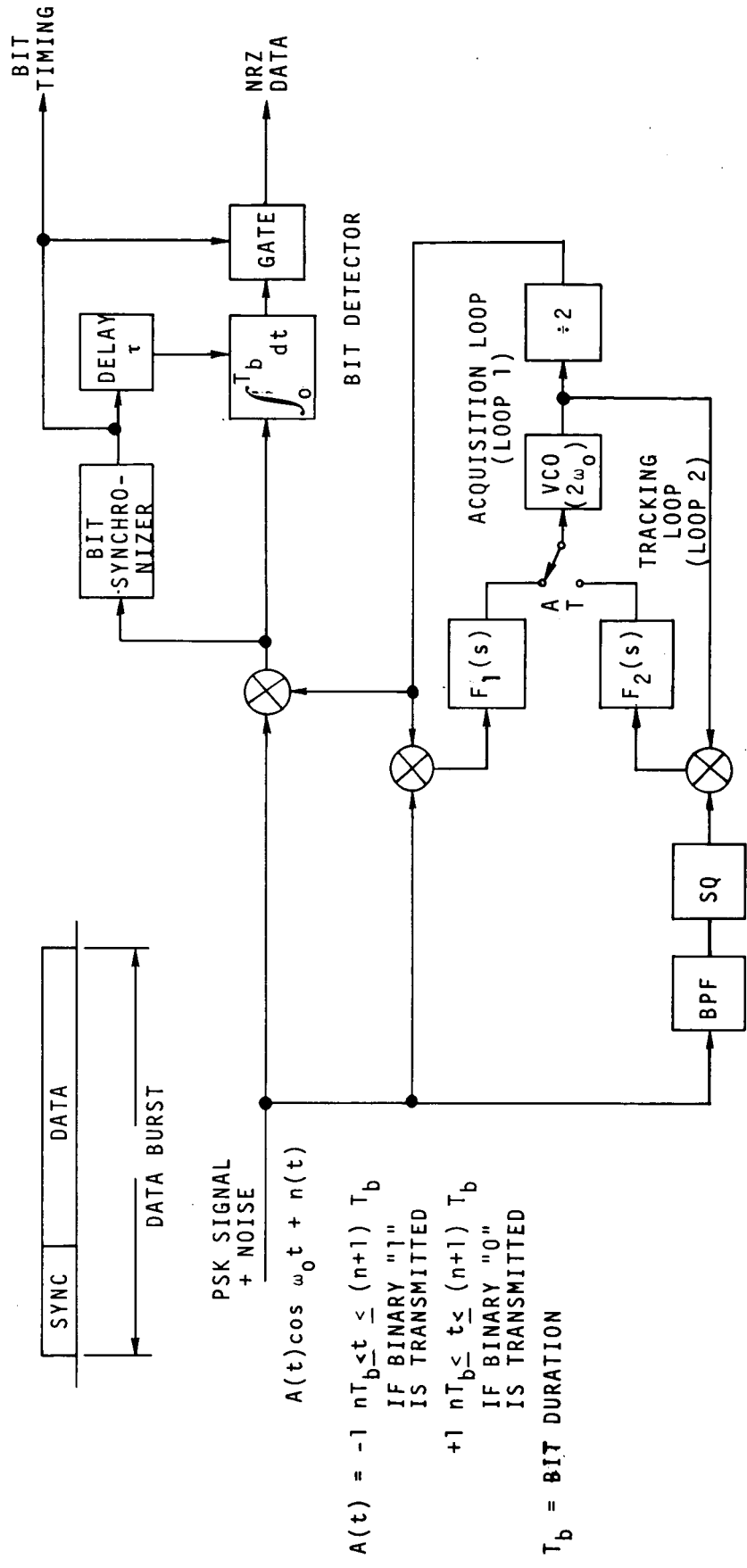
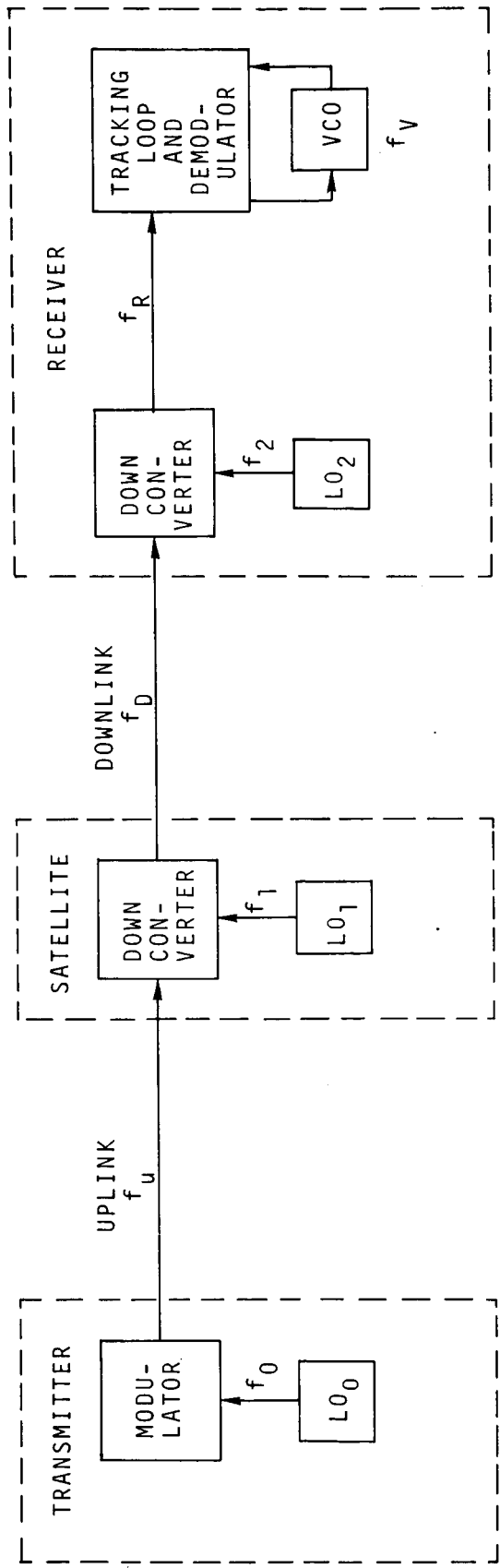


Figure A-2. General PSK Demodulator



$$\begin{aligned}
 f_{00} - \Delta f_0 &\leq f_0 \leq f_{00} + \Delta f_0 \\
 f_{01} - \Delta f_1 &\leq f_1 \leq f_{01} + \Delta f_1 \\
 f_{02} - \Delta f_2 &\leq f_2 \leq f_{02} + \Delta f_2 \\
 f_{0V} - \Delta f_V &\leq f_V \leq f_{0V} + \Delta f_V \\
 f_{0V} &= f_R
 \end{aligned}$$

$$\begin{aligned}
 f_u &= f_0 \\
 f_D &= f_0 - f_1 \\
 f_R &= (f_0 - f_1 - f_2) \\
 \Delta f_{\max} &= \max |f_R - f_V| = \max |f_0 - f_1 - f_2 - f_V| \\
 \Delta f_{\max} &= \Delta f_0 + \Delta f_1 + \Delta f_2 + \Delta f_V
 \end{aligned}$$

Figure A-3. Link Frequency Plan and Error Limits

Figure A-3, the frequency of the received signals from these two stations can be considered to be uncorrelated random variables, uniformly distributed between $f_R - \Delta f_R$ and $f_R + \Delta f_R$. If the frequency of the VCO in the tracking loop is uniformly distributed in the range $f_R - \Delta f_V \leq f_V \leq f_R + \Delta f_V$, then the maximum initial frequency error is $(\Delta f_R + \Delta f_V) = (\Delta f_0 + \Delta f_1 + \Delta f_2 + \Delta f_V)$. The initial frequency error once the system is operating can be considered as the frequency error between any two bursts. Since normally the frame length is much less than one second, the stability of the receiver VCO (S_V) and LO (S_2), and the satellite LO (S_1) over this short term can be considered to be very small (i.e., less than one part in 10^9). The long-term stability of the transmitter LO (S_0) may be on the order of one part in 10^7 . Thus, the maximum frequency error between any two bursts from different transmitters is given by:

$$\Delta f_{\max} = \left[(f_0 + S_0 f_0) - f_1 - f_2 - f_V \right] - \left[(f_0 - S_0 f_0) - (f_1 + S_1 f_1) - (f_2 + S_2 f_2) - (f_V + S_V f_V) \right]$$

$$\Delta f_{\max} = 2S_0 f_0 + S_V (f_1 + f_2 + f_V); S_1 = S_2 = S_V$$

for:

$$f_0 = 6 \times 10^9 \text{ Hz}, f_1 = 2 \times 10^9 \text{ Hz}, f_2 = 3.93 \times 10^9 \text{ Hz}$$

$$f_V = 7 \times 10^7 \text{ Hz}, S_0 = 10^{-7}, S_1 = S_2 = S_V = 10^{-9}$$

$$\begin{aligned} \Delta f_{\max} &= f_0 (2S_0 + S_V) = 6 \times 10^9 (2 \times 10^{-7} + 10^{-9}) \\ &= 1.21 \times 10^3 \text{ Hz} \end{aligned}$$

A.3 ACQUISITION TIME

First, the acquisition characteristics of the tracking loop alone will be analyzed. The parameters of this loop will be

determined primarily by the required phase jitter for demodulation. For demodulator performance, the parameter, δ , was defined as (Reference 2):

$$\delta \triangleq \frac{R}{B_L} \left[1 + \frac{N_O W}{2S} \right]^{-1} \approx \frac{R}{B_L}$$

$$\text{Thus, } B_L = \frac{R}{\delta} = \frac{\omega_n (1 + 4\zeta^2)}{8\zeta} \quad (\text{Reference 4})$$

Where ω_n is the natural loop frequency and ζ is the damping factor.

For a critically damped loop $\zeta = 1/\sqrt{2}$ and the above equation can be solved for ω_n :

$$\omega_n = \frac{4\sqrt{2}}{3} \frac{R}{\delta} = 1.89 \frac{R}{\delta}$$

Thus, the normalized initial conditions are:

$$\frac{\Delta\omega}{\omega_n} = \frac{2\pi\Delta f}{\omega_n} = 4 \times 10^3 \frac{\delta}{R}$$

$$\Delta\theta = -\pi$$

for the frequency error previously derived and the worst case phase error.

For a given $\Delta\theta$ and $\frac{\Delta\omega}{\omega_n}$, the acquisition time can be found from phase plane curves presented in Reference 9. From the curves, the acquisition time found is normalized in terms of time intervals of $1/4 \omega_n$.

The acquisition time can be expressed in terms of the number of bits as follows:

$$T_S = \frac{k}{4\omega_n}$$

where k = the number of time intervals measured on the phase plane plot. In general, k is a function of the initial conditions ($\frac{\Delta\omega}{\omega_n}$ and $\Delta\phi$). Substituting for ω_n ,

$$T_S = \frac{k\delta}{7.55R}$$

The number of bits required for carrier acquisition is thus:

$$n_S = T_S R = \frac{k\delta}{7.55}$$

In general, n_S is a function of the data rate R . If the maximum value of $\frac{\Delta\omega}{\omega_n}$ is less than 1, then the loop will achieve lock within n_S symbols for all values of data rate, $R > R_{\min}$ where R_{\min} is given by:

$$\frac{\Delta\omega}{\omega_n} = \frac{4 \times 10^3 \delta}{R_{\min}} = 1$$

$$R_{\min} = 4 \times 10^3 \delta$$

For $\delta \leq 10$ (which is the range of practical interest), $R_{\min} \leq 40$ kb/s. For the application of interest the baseband input data rates are on the order of 30 to 50 kb/s for a digital voice input and the burst data rates are 100 to 200 times as much, depending on the number of accesses. Therefore, R will always exceed R_{\min} and $\frac{\Delta\omega}{\omega_n} < 1$. Consequently, the worst case initial conditions $\Delta\phi = -\pi$ and $\frac{\Delta\omega}{\omega_n} = 1$ will be used. Under these assumptions, n_S is independent of R , and the value of k is approximately 25. Thus, the number of bits required for carrier recovery is given by:

$$n_S = \frac{k\delta}{7.55} = 3\delta$$

Thus, for the values of δ of interest, in the range from 2 to 5, n_S will be in the range from 6 to 15.

As was previously mentioned, a dual loop can be employed to reduce the acquisition time. Referring to Figure A-2, if the acquisition loop (i.e., loop containing $F_1(S)$) has a noise bandwidth of:

$$B_{L_1} = 3R,$$

then the settling time of this loop will be

$$T_{S_1} = \frac{1}{R}$$

or one symbol duration. The variance of the phase jitter of the acquisition loop is given by:

$$\begin{aligned} \sigma_1^2 &= \frac{N_o}{S} B_{L_1} \\ &= \frac{N_o}{E_b} \frac{B_{L_1}}{R} \\ &= \frac{3}{E_b/N_o} \end{aligned}$$

For $E_b/N_o \geq 5$, then $\sigma_1^2 \leq .6$

After the first symbol duration, the tracking loop (i.e., loop containing $F_2(S)$) is switched in and a second symbol duration is allowed to reduce the phase jitter to,

$$\sigma_2^2 = \left[\delta \frac{E_b}{N_o} \right]^{-1}$$

Thus, after two symbol durations, the information symbols can be demodulated.